

U.S. DEPARTMENT OF COMMERCE
National Technical Information Service

AD-A030 887

Pressure Distribution on the
Trailing Edge of an Airfoil
Oscillating in a Shear Layer

Aeronautical Research Associates of Princeton Inc N J

Prepared for

Air Force Office of Scientific Research, Bolling AFB, D C

Apr 76

UNCLASSIFIED

SECURITY CLASSIFICATION OF THIS PAGE (When Data Entered)

REPORT DOCUMENTATION PAGE		READ INSTRUCTIONS BEFORE COMPLETING FORM
1. REPORT NUMBER AFOSR - TR - 76 - 1076	2. GOVT ACCESSION NO.	3. RECIPIENT'S CATALOG NUMBER
4. TITLE (and Subtitle) PRESSURE DISTRIBUTION ON THE TRAILING EDGE OF AN OSCILLATING AIRFOIL IN A SHEAR LAYER		5. TYPE OF REPORT & PERIOD COVERED FINAL 1 Aug 75 - 31 Jan 76
		6. PERFORMING ORG. REPORT NUMBER A.R.A.P. Rept. No. 278
7. AUTHOR(s) JOHN E YATES		9. CONTRACT OR GRANT NUMBER(s) F44620-75-C-0010
		10. PROGRAM ELEMENT, PROJECT, TASK AREA & WORK UNIT NUMBERS 681307 9782-04 61102F
11. CONTROLLING OFFICE NAME AND ADDRESS AERONAUTICAL RESEARCH ASSOCIATES OF PRINCETON, INC 50 WASHINGTON ROAD PRINCETON, NEW JERSEY 08540		12. REPORT DATE April 1976
		13. NUMBER OF PAGES 56
14. MONITORING AGENCY NAME & ADDRESS (if different from Controlling Office)		15. SECURITY CLASS (of this report) UNCLASSIFIED
		15a. DECLASSIFICATION/DOWNGRADING SCHEDULE
16. DISTRIBUTION STATEMENT (of this Report) Approved for public release; distribution unlimited.		
17. DISTRIBUTION STATEMENT (of the abstract entered in Block 20, if different from Report)		
18. SUPPLEMENTARY NOTES		
19. KEY WORDS (Continue on reverse side if necessary and identify by block number) UNSTEADY AERODYNAMICS SHEAR LAYER TRAILING EDGE WIENER-HOPF		
20. ABSTRACT (Continue on reverse side if necessary and identify by block number) The problem of calculating the pressure distribution on an oscillating plate in a uniform parallel subsonic shear layer is idealized as a layer of fluid with constant velocity and temperature that are different from the free stream conditions. An approximate solution is developed with the Wiener-Hopf technique for the case that the shear layer velocity defect (displacement thickness/shear layer thickness) is small. The results are valid for arbitrary length scale of the surface deflection. The problem is a model of an airfoil trailing edge immersed in a fully developed turbulent layer and wake. The lowest-order steady		

UNCLASSIFIED

SECURITY CLASSIFICATION OF THIS PAGE (When Data Entered)

state solution is calculated for a linearly deflected flap and an exponential flap. Results for the linear flap agree with the known solution for a finite length air-foil. The lowest-order unsteady exponential flap and the first-order steady state exponential flap are also solved in detail. The first-order pressure decreases as the square root of the distance from the trailing edge like the lowest-order result, and in accordance with a full application of the Kutta condition. The amplitude of the correction is of order $\epsilon \sqrt{l}$ where ϵ is the ratio of the shear layer thickness to flap length. It is shown that the total lift on any section of the trailing edge of length L and flap length l increases like $(L/l)^2$ as L increases without bound in the absence of a shear layer. An experiment to determine how the shear layer limits the growth of lift is suggested.

1 (a)

UNCLASSIFIED

SECURITY CLASSIFICATION OF THIS PAGE (When Data Entered)

PREFACE

This report was prepared under Contract No. F44620-75-C-0010 to the Air Force Office of Scientific Research. The program technical monitor was Mr. W. Walker. The principal investigator was Dr. John E. Yates.

REVISIONS		
175	None	<input checked="" type="checkbox"/>
176	None	<input type="checkbox"/>
177	None	<input type="checkbox"/>

A

OCT 19 1976
LIBRARY
D

TABLE OF CONTENTS

<u>Section</u>		
I.	INTRODUCTION.....	1
II.	FORMULATION OF THE TRAILING EDGE PROBLEM..	3
	Statement of the Problem.....	3
	Basic Equations.....	3
	Boundary Conditions.....	5
	Comments.....	6
III.	SOLUTION OF THE TWO-LAYER MODEL.....	9
	The Reduced Problem.....	9
	Application of Wiener-Hopf.....	12
	Exact Inviscid Solution.....	14
	An Integral Equation for $Q(\alpha)$	15
	Analysis of ε	17
IV.	APPLICATIONS.....	22
	The Steady State Linear Flap.....	22
	Remarks	24
	The Exponential Flap (Zero Order).....	24
	First-Order Exponential Flap (Steady State).....	30
	Asymptotic Results.....	34
	The Paradox of Infinite Lift - A Suggested Experiment.....	35
	The Unsteady Trailing Edge.....	37
V.	CONCLUSIONS.....	38
	REFERENCES.....	39
	APPENDIX	
A	EVALUATION OF $N_1(x)$ and $N_2(x)$	40
B	ASYMPTOTIC ANALYSIS OF $F^*(z, \varepsilon)$	42

NOMENCLATURE

a	a^2_{∞} local speed of sound
a_{∞}	free stream speed of sound
$\frac{D}{Dt}$	$V \frac{\partial}{\partial x} + \frac{\partial}{\partial t}$
$\frac{D}{Dx}$	$V \frac{\partial}{\partial x} + i\omega$
$E_1(z)$	exponential integral, see (4.39)
$E_1(z)$	see (4.41)
$f(x)$	surface deflection, $x < 0$
$F(z)$	Dawson's integral, see (4.18)
$F(z, \epsilon)$	generalized Dawson's integral, see (4.27) and Appendix B
$G(z)$	see (4.15) and (4.16)
$H(x)$	Heaviside step function
i	$\sqrt{-1}$
l	scale factor in exponential flap, see (4.5) and (4.7)
M	V/a local Mach number
M_{∞}	V_{∞}/a_{∞} free stream Mach number
$N_1(x), N_2(x)$	see (3.21) and Appendix A
$N_2(\alpha)$	see (3.20)
p	perturbation pressure/free stream density
$p_0(x)$	lowest-order pressure, see (3.21)
$p'(x)$	first-order pressure correction, see (3.36)
$P(x), P'(x)$	see (3.36) through (3.38)
$Q_0^*(x)$	see (3.30)
$Q_0(\alpha)$	lowest-order solution for $Q(\alpha)$, see (3.26)
$Q'(\alpha)$	first-order correction to $Q_0(\alpha)$, see (3.33)

$Q(\alpha)$	unknown, in dual integral equations, see (3.23)
t	time
$V(y)$	shear layer mean velocity profile
V_w	shear layer velocity at the wall
w	vertical fluid velocity
$W(x)$	downwash function, $x < 0$, see (2.15)
x_h	hinge location of linear flap, see (4.1) and Fig. 5
x, y	Cartesian coordinates, see Fig. 1
α	Fourier transform variable
α_1, α_2	see (3.5)
$\alpha_1^{\infty}, \alpha_2^{\infty}$	see (7.10)
B	$(1 - M^2)^{1/2}$
B_{∞}	$(1 - M_{\infty}^2)^2$
γ	.57721 Euler's constant
$\bar{\gamma}$	shear layer correction factor, see (4.34)
Γ	see (2.6) and Fig. 2
Γ_{∞}	value of Γ in free stream, see (2.8) and Fig. 2
δ	shear layer thickness
δ^*	shear layer displacement thickness, see (3.47)
$\delta(x)$	Dirac delta function
Δ	δ^*/δ , see (4.36)
ϵ	$2\theta\delta/\xi$
$\bar{\epsilon}^*(x)$	see (3.38)
$\theta(y)$	shear layer normalized mean temperature profile
ρ_{∞}	free stream density
σ	see (3.9)

$\Sigma(\alpha)$	see (3.8) and Fig. 4
ϕ	flap deflection angle, see (4.1) and (4.5)
ω	radian frequency of simple harmonic motion
$(\bar{\quad})$	denotes Fourier transform amplitude of any variable
$(\dot{\quad})$	denotes ordinary differentiation with respect to y
\cdot	sub- or superscript to denote free stream value
Im	imaginary part of a complex quantity
Re	real part of a complex quantity

I. INTRODUCTION

In a previous long-range effort (see Ref. 1,2) under Air Force sponsorship, the author has developed an integral approach for including the effect of the boundary layer in the conventional unsteady aerodynamic analysis. The original objective of the program was to develop the theory to a point where it could be used in the analysis of supersonic panel flutter. This objective has been accomplished. The integral technique has been successfully integrated into a panel flutter computer program (Refs. 3,4,5) under Air Force and NASA sponsorship. The effect of the boundary layer on panel flutter has been calculated and compared with experimental results. The agreement is remarkably good.

Because of the success of the integral approach in solving the panel flutter problem, a shorter range program was initiated to investigate related applications of the theory. The particular problem of noise generation and/or reflection by a panel surface in a shear layer was a possible source of application. The trailing edge problem was a second possibility. Our work on the acoustic problem has resulted in a revolutionary new theory of aerodynamic sound generation. This work is reported in two published documents (see Refs. 6,7). Our final report is concerned solely with the trailing edge problem.

To the author's knowledge, the first work on the application of shear layer aerodynamic theory to lifting surface problems is due to Dowell and Ventres (Ref. 8). In a subsequent study, Ventres (Ref. 9) developed the shear layer kernel function in detail for steady incompressible flow and calculated the effect of the shear layer on the lift curve slope and center of pressure of various two- and three-dimensional airfoils. He showed that the lift curve slope is decreased while the center of pressure is unaffected by the shear layer. In a related study, Williams (Ref. 10) has developed a general approach for solving a generalized class of singular integral equations that result when the shear layer is introduced into the usual aerodynamic theory. More recently, Dowell, Chi and Williams

(Ref. 11) have been attempting to extend the kernel function concept to unsteady flow by expanding for small frequency about the steady-state solution of Ventres.

The present work is closely related to the work of Dowell and his co-workers in that we start with the same basic model of the shear layer and focus on the solution of a lifting surface problem as opposed to the panel aerodynamic problem. Our approach is somewhat different, however, in that we attempt the development of an analytic solution for a very special airfoil and shear layer model. Specifically, we treat a semi-infinite airfoil and replace the actual shear layer by a flow with constant velocity and temperature that are different from the free stream conditions. An approximate solution is developed with the Wiener-Hopf technique in the limit of small shear layer velocity defect. Explicit results are given for the case of a linearly deflected flap and an exponential flap. The analytic results should be useful for evaluating our integral approach and other approximate schemes for solving kernel function models.

II. FORMULATION OF THE TRAILING EDGE PROBLEM

Statement of the Problem

We consider the problem illustrated in Fig. 1. A two-dimensional flat plate extends along the negative axis with a trailing edge at the origin. The plate undergoes small oscillations. The flow is uniform subsonic except in a thin layer of thickness δ near the x-axis where the mean velocity is a function of y only. The basic problem is to determine the pressure distribution on the plate.

The model problem we have adopted is an idealization of the trailing edge of an oscillating airfoil. The primary aim is to determine the effect of the shear layer on the surface pressure near the trailing edge. The solution of the corresponding inviscid problem is known (Ref. 12) and is readily obtained with the Wiener-Hopf technique. In the present work we show how the same technique can be used to obtain an approximate solution for a simple two-layer model of the shear layer.

Basic Equations

The equations for the perturbation pressure p and vertical velocity w are (Ref. 1) in dimensional form:

$$\frac{1}{a_\infty^2} \frac{D^2 p}{Dt^2} - \text{div} (\theta \text{ grad } p) = 2V' \frac{\partial w}{\partial x} \quad (2.1)$$

$$\frac{Dw}{Dt} + \theta \frac{\partial p}{\partial y} = 0 \quad (2.2)$$

where

$$p = \frac{p'}{\rho_\infty} \quad \text{perturbation pressure/density}$$

$$a_\infty = \quad \text{free stream sound speed}$$

$$\frac{D}{Dt} = V \frac{\partial}{\partial x} + \frac{\partial}{\partial t}$$

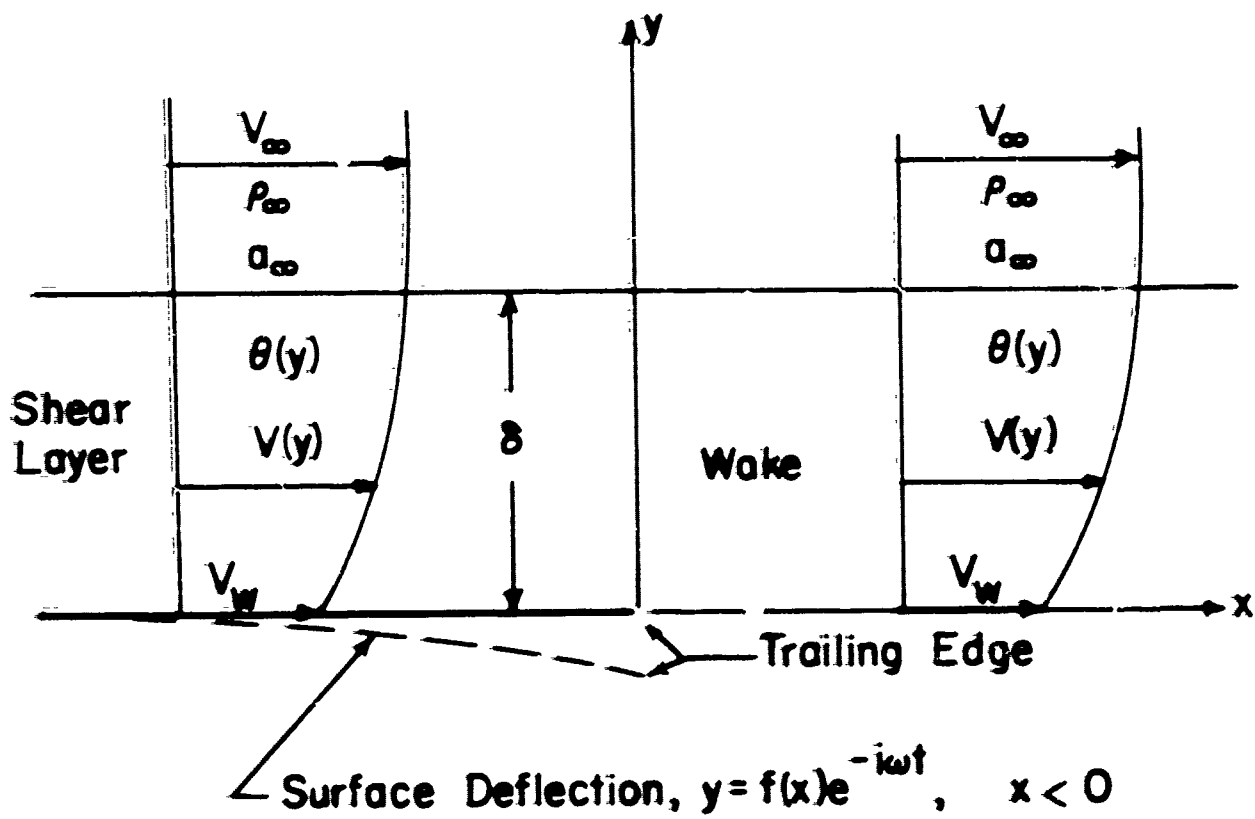


Fig. 1. Geometry of the Trailing Edge Problem

$$\begin{aligned}
 V &= V(y) && \text{shear layer velocity profile} \\
 \theta &= \frac{T_0(y)}{T_\infty} && \text{normalized temperature profile in the} \\
 &&& \text{shear layer}
 \end{aligned}
 \tag{2.3}$$

We assume the motion of the plate to be simple harmonic in time ($q \rightarrow qe^{-i\omega t}$) so that p and w are simple harmonic at every point in space. Furthermore, we Fourier analyze the x dependence of each dependent variable. Thus,

$$\begin{aligned}
 \bar{q}(\alpha) &= \frac{1}{(2\pi)^{1/2}} \int_{-\infty}^{\infty} dx e^{i\alpha x} q(x) \\
 \text{and} \\
 q(x) &= \frac{1}{(2\pi)^{1/2}} \int_{-\infty}^{\infty} dx e^{-i\alpha x} \bar{q}(\alpha)
 \end{aligned}
 \tag{2.4}$$

where q is either p or w . The equations for the Fourier amplitudes become

$$\begin{aligned}
 i(\alpha V + \omega) \frac{d\bar{w}}{dy} - i\alpha V \bar{w} &= \theta \Gamma^2 \bar{p} \\
 \frac{d\bar{p}}{dy} &= i \frac{(\alpha V + \omega)}{\theta} \bar{w}
 \end{aligned}
 \tag{2.5}$$

where

$$\Gamma^2 = \alpha^2 - \frac{(\alpha V + \omega)^2}{a_\infty^2 \theta}
 \tag{2.6}$$

Boundary Conditions

In the region outside the shear layer (see Fig. 1) we obtain a single equation for \bar{p} ; i.e.,

$$\frac{d^2 \bar{p}}{dy^2} - \Gamma_\infty^2 \bar{p} = 0
 \tag{2.7}$$

where

$$\Gamma_\infty = \left[\alpha^2 - \frac{(\alpha V_\infty + \omega)^2}{a_\infty^2} \right]^{1/2}
 \tag{2.8}$$

We require that the pressure either decays exponentially or corresponds to outgoing (acoustic) waves. Thus,

$$\bar{p} \rightarrow Ae^{-\Gamma_\infty y} \quad \text{for } y \rightarrow \infty \quad (2.9)$$

and the boundary condition is satisfied if we choose the branch cuts for the complex function $\Gamma_\infty(\alpha)$ as shown in Fig. 2. The branch points α_1 and α_2 are

$$\alpha_1^\infty = + \frac{\omega}{a_\infty - V_\infty} \quad , \quad \alpha_2^\infty = - \frac{\omega}{a_\infty + V_\infty} \quad (2.10)$$

and

$$\Gamma_\infty = \beta_\infty (\alpha - \alpha_1^\infty)^{1/2} (\alpha - \alpha_2^\infty)^{1/2} \quad (2.11)$$

$$\beta_\infty = (1 - M_\infty^2)^{1/2} \quad (2.12)$$

For reasons that will become clear later, we assume that ω has a small positive complex part so that α_1 is slightly above the real axis and α_2 is slightly below the real axis as indicated in Fig. 2. On the real axis we can write

$$\begin{aligned} \Gamma_\infty &= \beta_\infty |\alpha - \alpha_1^\infty|^{1/2} |\alpha - \alpha_2^\infty|^{1/2} && \alpha > \alpha_1^\infty \\ &&& \text{or } \alpha < \alpha_2^\infty \\ &= -i\beta_\infty |\alpha - \alpha_1^\infty|^{1/2} |\alpha - \alpha_2^\infty|^{1/2} && \alpha_2^\infty < \alpha < \alpha_1^\infty \end{aligned} \quad (2.13)$$

which results satisfy the required boundary condition for $y \rightarrow \infty$.

Additional boundary conditions in the shear layer are the following. The pressure must be continuous at all points. If the mean flow properties are continuous, then the velocity w is also continuous. If we admit a discontinuity in V , then continuity of particle position requires that

$$(\alpha V_+ + \omega)\bar{w}_- = (\alpha V_- + \omega)\bar{w}_+ \quad (2.14)$$

where the + and - subscripts refer to the points slightly above or below the y location of the discontinuity.

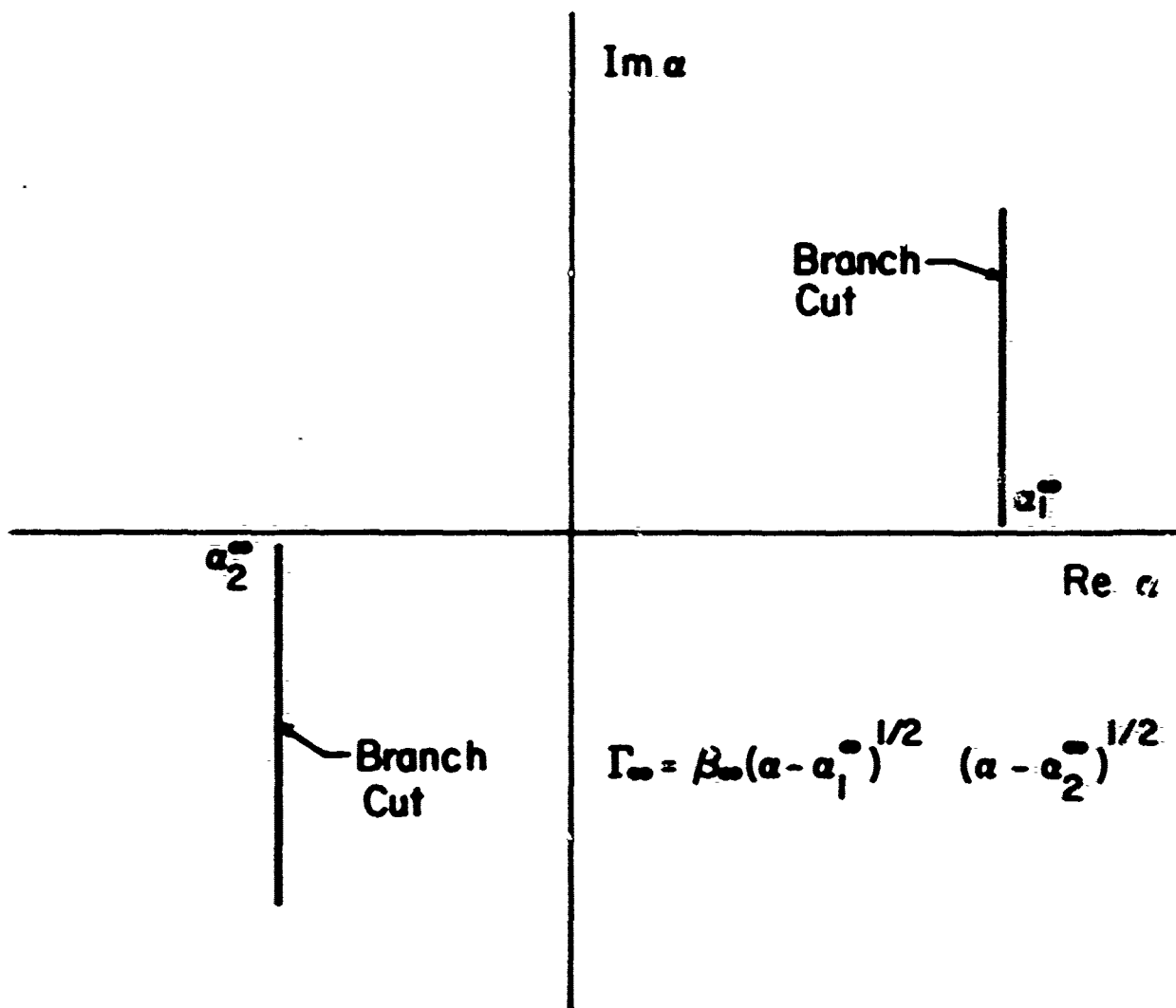


Fig. 2. Definition of $\Gamma_\infty(\alpha)$; (Also see $\Gamma(\alpha)$, Eq. (3.5).

The boundary conditions on the x axis are as follows:

$$w(x,0) = W(x) = V_w \frac{\partial f}{\partial x} + i\omega f \quad \text{for } x < 0 \quad (2.15)$$

$$p(x,0) = 0 \quad \text{for } x > 0 \quad (2.16)$$

where $f(x)$ is the deflection of the plate. Finally, we require that the pressure tend to zero at the trailing edge of the plate. Thus, we have invoked a form of the Kutta condition.

Comments

The solution of the problem thus formulated is difficult for an arbitrary shear layer profile, Mach number, frequency, etc. Thus, we consider a simplified problem by choosing a two-step shear profile as shown in the next section. We remark that other simplifications can also be made. For example, in the incompressible case we have

$$\theta = 1$$

$$\Gamma^2 = \alpha^2 - \omega^2/a_\infty^2 \quad (2.17)$$

and from (2.5) we find that

$$\frac{d^2 \bar{w}}{dz^2} - \left(\frac{\alpha V}{\alpha V + \omega} + \Gamma^2 \right) \bar{w} = 0 \quad (2.18)$$

For a linear velocity profile, the equation for \bar{w} can be solved exactly in terms of exponential function and the pressure follows by integration. Recently, Goldstein (Ref. 13) has considered the compressible problem for which there is also an exact solution for a linear velocity profile.

III. SOLUTION OF THE TWO-LAYER MODEL

The Reduced Problem

We consider the simplified shear layer shown in Fig. 3. The velocity and temperature are assumed to be constant in a layer of thickness δ . Free stream conditions hold for $y > \delta$.

In the layer the pressure \bar{p} satisfies the ordinary differential equation.

$$\frac{d^2 \bar{p}}{dy^2} - \Gamma^2 \bar{p} = 0 \quad (3.1)$$

where

$$\Gamma = \left[\alpha^2 - \frac{(\alpha V + \omega)^2}{a^2} \right]^{1/2} \quad (3.2)$$

$$a^2 = a_{\alpha 0}^2 \quad \text{speed of sound in the layer} \quad (3.3)$$

The solution of (3.1) is

$$\bar{p} = B e^{-\Gamma y} + C e^{\Gamma y} \quad 0 < y < \delta \quad (3.4)$$

where the definition of Γ in the complex α -plane is precisely the same as for Γ_{∞} (see Fig. 2). We have

$$\Gamma = \beta (\alpha - \alpha_1)^{1/2} (\alpha - \alpha_2)^{1/2}$$

$$\beta = (1 - M^2)^{1/2}$$

$$M = V/a$$

$$\alpha_1 = \frac{\omega}{a - V}$$

$$\alpha_2 = -\frac{\omega}{a + V} \quad (3.5)$$

The velocity in the layer follows by differentiation of (3.4) and use of (2.5); i.e.,

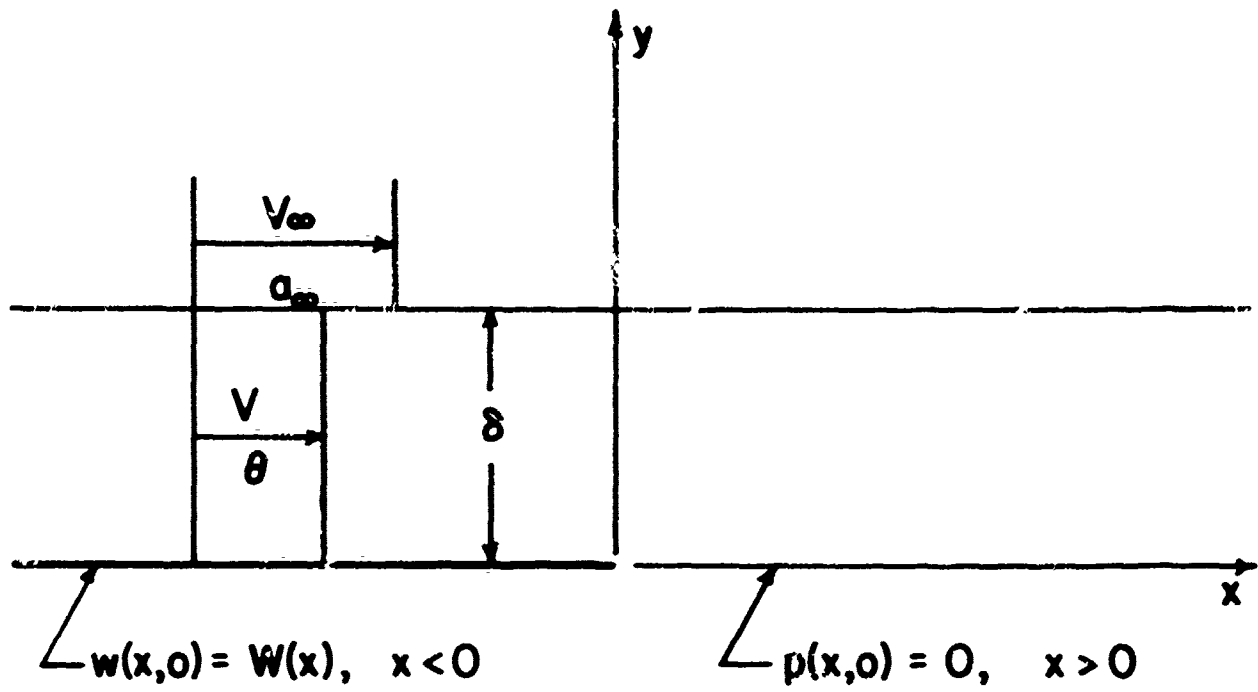


Fig. 3. The Two-Step Shear Layer Model

$$\bar{w} = i\theta\Gamma(Be^{-\Gamma y} - Ce^{\Gamma y})/(\alpha V + \omega) \quad 0 < y < \delta \quad (3.6)$$

For $y > \delta$, we have (see (2.9))

$$\bar{p} = Ae^{-\Gamma_{\alpha} y}$$

$$\bar{w} = \frac{iA e^{-\Gamma_{\alpha} y}}{V + \omega} \quad (3.7)$$

The pressure and particle position must be continuous at $y = \delta$. (Note (2.14).) We thus solve for B and C in terms of A and finally calculate the ratio

$$\frac{C}{B} \equiv \Sigma = \sigma e^{-2\Gamma\delta} \quad (3.8)$$

where

$$\sigma = \frac{\Gamma\theta(\alpha V_{\infty} + \omega)^2 - \Gamma_{\infty}(\alpha V + \omega)^2}{\Gamma\theta(\alpha V_{\infty} + \omega)^2 + \Gamma_{\infty}(\alpha V + \omega)^2} \quad (3.9)$$

For $y = 0$, we get from (3.4) and (3.6)

$$\bar{p} = (1 + \Sigma)B(\alpha)$$

$$-i \frac{(\alpha V + \omega)}{\theta} \bar{w} = \Gamma(1 - \Sigma)B(\alpha) \quad (3.10)$$

we formally invert this pair of equations to obtain

$$p(x) = \frac{1}{(2\pi)^{1/2}} \int_{-\infty}^{\infty} e^{-i\alpha x} (1 + \Sigma) \cdot B(\alpha) \cdot d\alpha \quad (3.11)$$

$$\frac{1}{\theta} \frac{Dw}{Dx} = \frac{1}{(2\pi)^{1/2}} \int_{-\infty}^{\infty} e^{-i\alpha x} \Gamma \cdot (1 - \Sigma) \cdot B(\alpha) \cdot d\alpha \quad (3.12)$$

where

$$\frac{D}{Dx} = V \frac{\partial}{\partial x} + i\omega \quad (3.13)$$

These are the basic equations that we use to study the trailing edge problem. The function $B(\alpha)$ is the essential unknown. We have cast the problem in the above form to facilitate application of the Wiener-Hopf technique. In the complete absence of a shear layer we have $\Sigma = 0$ and Wiener-Hopf solves the problem exactly as we shall see below.

Application of Wiener-Hopf

We apply the boundary conditions on the x-axis (see (2.15) and (2.16)) to obtain the following pair of dual integral equations:

$$\frac{1}{(2\pi)^{1/2}} \int_{-\infty}^{\infty} e^{-i\alpha x} (1 + \Sigma) B(\alpha) d\alpha = 0, \quad x > 0 \quad (3.14)$$

$$\frac{1}{(2\pi)^{1/2}} \int_{-\infty}^{\infty} e^{-i\alpha x} (1 - \Sigma) B(\alpha) d\alpha = \frac{1}{\theta} \frac{DW}{Dx}, \quad x < 0 \quad (3.15)$$

Next, we follow the Jones method of applying the Wiener-Hopf technique (see Ref. 12) to partially symmetrize the integrands in (3.14) and (3.15). First, we replace x by $x + \xi$ in (3.14), multiply by "some function" $N_1(\xi)$ and integrate from 0 to ∞ . We get

$$\frac{1}{(2\pi)^{1/2}} \int_{-\infty}^{\infty} e^{-i\alpha x} N_-(\alpha) (1 + \Sigma) B(\alpha) d\alpha = 0, \quad x > 0 \quad (3.16)$$

where

$$N_-(\alpha) = \int_0^{\infty} e^{-i\alpha x} N_1(x) dx \quad (3.17)$$

and $N_-(\alpha)$ must be analytic in "some" lower half of the complex plane. Similarly, we replace x by $x - \xi$ in (3.15), multiply by "some function" $N_2(\xi)$ and integrate to obtain

$$\begin{aligned} \frac{1}{(2\pi)^{1/2}} \int_{-\infty}^{\infty} e^{-i\alpha x} N_+(\alpha) \Gamma(1 - \Sigma) B(\alpha) d\alpha \\ = \int_0^{\infty} N_2(\xi) \left[\frac{1}{\theta} \frac{DW}{D\eta} \right]_{x-\xi} d\xi, \quad x < 0 \end{aligned} \quad (3.18)$$

where

$$N_+(\alpha) = \int_0^{\infty} e^{i\alpha x} N_1(x) dx \quad (3.19)$$

and $N_+(\alpha)$ is analytic in "some" upper half of the complex plane.

Next, we construct the functions $N_1(x)$ and $N_2(x)$ by choosing

$$\begin{aligned} N_-(\alpha) &= 1/(\alpha - \alpha_1)^{1/2} \\ N_+(\alpha) &= 1/(\alpha - \alpha_2)^{1/2} \end{aligned} \quad (3.20)$$

where α_1 and α_2 are the branch points of the function $\Gamma(\alpha)$ (see (3.5) and Fig. 2). Note that $N_-(\alpha)$ is analytic in the lower half plane ($\text{Im } \alpha < \text{Im } \alpha_1$) and $N_+(\alpha)$ is analytic in the upper half plane ($\text{Im } \alpha > \text{Im } \alpha_2$). It is essential for the analytic continuation used in the Wiener-Hopf technique that these two half planes overlap. This was the reason for assuming a small positive complex part of ω . We also remark that the particular choice for $N_-(\alpha)$ and $N_+(\alpha)$ establishes the character of the pressure near the trailing edge. We shall see that $p(x)$ tends to zero as $\sqrt{-x}$ for $x \rightarrow 0^-$ in accordance with the Kutta condition.

With (3.20) the functions $N_1(x)$ and $N_2(x)$ are easily evaluated (see Appendix A). We get

$$\begin{aligned} N_1(x) &= (\pi x)^{-1/2} e^{i\alpha_1 x + i\pi/4}, \quad x > 0 \\ N_2(x) &= (\pi x)^{-1/2} e^{-i\alpha_2 x - i\pi/4}, \quad x > 0 \end{aligned} \quad (3.21)$$

Both N_1 and N_2 are zero for $x < 0$.

Finally, we multiply (3.16) by $e^{i\alpha_1 x}$ and differentiate with respect to x . Our dual integral equations (3.14) and (3.15) are reduced to the following:

$$\frac{1}{(2\pi)^{1/2}} \int_{-\infty}^{\infty} e^{-i\alpha x} (1 + \Sigma) Q(\alpha) d\alpha = 0, \quad x > 0 \quad (3.22)$$

$$\begin{aligned} \frac{1}{(2\pi)^{1/2}} \int_{-\infty}^{\infty} e^{-i\alpha x} (1 - \Sigma) Q(\alpha) d\alpha \\ = \frac{1}{\beta\theta} \int_0^{\infty} N_2(\xi) \left[\frac{DW}{Dn} \right]_{x-\xi} d\xi, \quad x < 0 \end{aligned} \quad (3.23)$$

where

$$Q(\alpha) = (\alpha - \alpha_1)^{1/2} B(\alpha) \quad (3.24)$$

Once $Q(\alpha)$ is known, the wall pressure is calculated with

$$p(x) = \frac{1}{(2\pi)^{1/2}} \int_{-\infty}^{\infty} e^{-i\alpha x} \frac{(1 + \Sigma) Q(\alpha)}{(\alpha - \alpha_1)^{1/2}} d\alpha \quad (3.25)$$

Exact Inviscid Solution

In the absence of any shear defect, we have $\Sigma = 0$ and the pair (3.22) and (3.23) yield the exact solution of the problem; i.e.,

$$Q_0(\alpha) = \frac{1}{(2\pi)^{1/2}} \int_{-\infty}^0 e^{i\alpha x} dx \cdot \frac{1}{\beta\theta} \int_0^{\infty} N_2(\xi) \left[\frac{DW}{Dn} \right]_{x-\xi} d\xi \quad (3.26)$$

where $\beta = \beta_{\infty}$ and $\theta = 1$. For the surface pressure we get

$$p_0(x) = \frac{1}{(2\pi)^{1/2}} \int_{-\infty}^{\infty} e^{-i\alpha x} \cdot \frac{Q_0(\alpha)}{(\alpha - \alpha_1)^{1/2}} d\alpha, \quad x < 0 \quad (3.27)$$

We can reduce these results further with the convolution integral. For (3.27) we get

$$p_0(x) = \int_x^c N_1(\xi - x) Q_0^*(\xi) d\xi, \quad x < 0 \quad (3.28)$$

where

$$Q_0^*(\xi) = \frac{1}{(2\pi)^{1/2}} \int_{-\infty}^{\infty} e^{-i\alpha\xi} Q_0(\alpha) d\alpha, \quad \xi < 0 \quad (3.29)$$

Now substitute (3.26) into (3.29) and invert the order of integration to get

$$Q_0^*(x) = \frac{1}{8\theta} \int_0^{\infty} N_2(\xi) \left[\frac{DW}{D\eta} \right]_{x-\xi} d\xi, \quad x < 0 \quad (3.30)$$

Thus, the exact pressure on the surface becomes

$$p_0(x) = \frac{1}{8\theta} \int_x^c N_1(s - x) ds \int_0^{\infty} N_2(\xi) \left[\frac{DW}{D\eta} \right]_{s-\xi} d\xi \quad (3.31)$$

where N_1 and N_2 are defined by (3.21).

For any specific downwash distribution, $W(x)$, the calculation of $p_0(x)$ has been reduced to a double quadrature. We consider specific examples in the subsequent section.

An Integral Equation for $Q(\alpha)$

The obstacle that prohibits the exact solution for $Q(\alpha)$ in (3.22) and (3.23) is the complex function $\Sigma(\alpha)$. We can disguise our difficulty somewhat by transposing the two terms that contain Σ to the right-hand side of the equation and formally inverting. The result is a singular integral equation for the unknown $Q(\alpha)$; i.e.,

$$Q(\alpha) = Q_0(\alpha) - \frac{1}{i\pi} \int_{-\infty}^{\infty} \frac{\Sigma(\alpha') Q(\alpha')}{\alpha' - \alpha} d\alpha' \quad (3.32)$$

where $Q_0(\alpha)$ is given by (3.30) and the integral is a standard Hilbert transform (Cauchy principal value integral).

Since we still do not know $Q(\alpha)$, we have only reduced two integral equations to one with the last trick. However, the form of (3.28) suggests that we might iterate for Q . If $\Sigma(\alpha)$ is in some sense small, we can expect to obtain useful results. We postpone the investigation of Σ for a moment and formally derive a first-order result. We have to first order in Σ

$$Q_1 = Q_0 + Q'$$

and

$$Q' = -\frac{1}{i\pi} \int_{-\infty}^{\infty} \frac{\Sigma(\alpha') Q_0(\alpha')}{\alpha' - \alpha} d\alpha' \quad (3.33)$$

Next, we evaluate the first-order pressure with (3.25). We have

$$(1 + \Sigma)Q_1 = (1 + \Sigma)Q_0 + Q' + O(\Sigma^2) \quad (3.34)$$

and we write the pressure in the form of a convolution integral. Thus,

$$p_1(x) = \int_x^{\infty} P(\xi) N_1(\xi - x) d\xi \quad (3.35)$$

where

$$P(x) = \frac{1}{(2\pi)^{1/2}} \int_{-\infty}^{\infty} e^{-i\alpha x} [(1 + \Sigma)Q_0 + Q'] d\alpha \quad (3.36)$$

Consider

$$\begin{aligned} P'(x) &= \frac{1}{(2\pi)^{1/2}} \int_{-\infty}^{\infty} e^{-i\alpha x} Q'(\alpha) d\alpha \\ &= \frac{1}{(2\pi)^{1/2}} \int_{-\infty}^{\infty} \Sigma(\alpha') Q_0(\alpha') d\alpha' \cdot \frac{1}{i\pi} \int_{-\infty}^{\infty} \frac{e^{-i\alpha x}}{\alpha - \alpha'} d\alpha \\ &= \frac{\text{sgn}(-x)}{(2\pi)^{1/2}} \int_{-\infty}^{\infty} e^{-i\alpha x} \Sigma(\alpha) Q_0(\alpha) d\alpha \end{aligned} \quad (3.37)$$

Thus,

$$P(x) = \frac{1}{(2\pi)^{1/2}} \int_{-\infty}^{\infty} e^{-i\alpha x} (1 + 2\Sigma) Q_0(\alpha) d\alpha \quad x < 0$$

$$= 0 \quad , \quad x > 0 \quad (3.38)$$

and

$$p_1(x) = p_0(x) + p'(x) \quad , \quad x < 0 \quad (3.39)$$

where $p_0(x)$ is given by (3.31) and

$$p'(x) = \int_x^0 P'(\xi) N_1(\xi - x) d\xi \quad , \quad x < 0 \quad (3.40)$$

with

$$P'(x) = \frac{2}{(2\pi)^{1/2}} \int_{-\infty}^{\infty} e^{-i\alpha x} \Sigma(\alpha) Q_0(\alpha) d\alpha$$

$$= \frac{2}{(2\pi)^{1/2}} \int_{-\infty}^0 Q_0^*(\xi) \Sigma^*(x - \xi) d\xi \quad x < 0 \quad (3.41)$$

where Q_0^* is defined by (3.30) and

$$\Sigma^*(x) = \frac{1}{(2\pi)^{1/2}} \int_{-\infty}^{\infty} e^{-i\alpha x} \Sigma(\alpha) d\alpha \quad , \quad x < 0 \quad (3.42)$$

The first-order pressure is zero for $x > 0$ and providing $P(x)$ is regular at the origin, $p_1(x)$ should vanish for $x \rightarrow 0^-$ at the trailing edge.

Analysis of Σ

The first-order result will be useful to study the effect of the shear layer on the trailing edge pressure providing the correction is bounded. The magnitude of the correction is determined completely by the magnitude of Σ . We turn now to a brief analysis of Σ that we rewrite here for convenience (see (3.8) and (3.9)).

$$\Sigma = \sigma e^{-2\Gamma\delta}$$

$$\sigma = \frac{\Gamma\theta(\alpha V_\infty + \omega)^2 - \Gamma_\infty(\alpha V + \omega)^2}{\Gamma\theta(\alpha V_\infty + \omega)^2 + \Gamma_\infty(\alpha V + \omega)^2} \quad (3.43)$$

where

$$\begin{aligned} \Gamma &= \beta(\alpha - \alpha_1)^{1/2}(\alpha - \alpha_2)^{1/2} \\ \Gamma_\infty &= \beta_\infty(\alpha - \alpha_1^\infty)^{1/2}(\alpha - \alpha_2^\infty)^{1/2} \end{aligned} \quad (3.44)$$

with

$$\begin{aligned} \alpha_1 &= \frac{\omega}{a - V} & \alpha_2 &= -\frac{\omega}{a + V} \\ \alpha_1^\infty &= \frac{\omega}{a_\infty - V_\infty} & \alpha_2^\infty &= -\frac{\omega}{a_\infty + V_\infty} \end{aligned} \quad (3.45)$$

We first examine the relative magnitude of the branch points for the case of an adiabatic wall; i.e.,

$$a^2 + \frac{\gamma - 1}{2} V^2 = a_\infty^2 + \frac{\gamma - 1}{2} V_\infty^2 \quad (3.46)$$

and

$$a = a_\infty \left[1 + \frac{\gamma - 1}{4} M_\infty^2 (1 - V^2/V_\infty^2) \right] \quad (3.47)$$

Thus,

$$a - V = (a_\infty - V_\infty) \left[1 + \frac{M_\infty}{1 - M_\infty} \left(1 - \frac{V}{V_\infty} \right) \left\{ 1 + \frac{\gamma - 1}{4} M_\infty \left(1 + \frac{V}{V_\infty} \right) \right\} \right]$$

and

$$\begin{aligned} \alpha_1 &= \frac{\omega}{a - V} = \alpha_1^\infty \left[1 - \left(1 - \frac{V}{V_\infty} \right) \frac{M_\infty}{1 - M_\infty} \left\{ 1 + \frac{\gamma - 1}{4} M_\infty \left(1 + \frac{V}{V_\infty} \right) \right\} \right] \\ &\leq \alpha_1^\infty \end{aligned} \quad (3.48)$$

Similarly, we find that

$$\begin{aligned} \alpha_2 &= -\frac{\omega}{a + V} = \alpha_2^\infty \left[1 + \left(1 - \frac{V}{V_\infty} \right) \frac{M_\infty}{1 + M_\infty} \left\{ 1 - \frac{\gamma - 1}{4} M_\infty \left(1 + \frac{V}{V_\infty} \right) \right\} \right] \\ &\leq \alpha_2^\infty \quad \text{since } \alpha_2^\infty \text{ is negative} \end{aligned} \quad (3.49)$$

It follows by inspection of (3.43) that

$$\begin{aligned}\sigma(\alpha_{1,2}) &= -1, & \sigma(\alpha_{1,2}^{\infty}) &= +1 \\ \sigma(-w/V_{\infty}) &= -1, & \sigma(-w/V) &= +1\end{aligned}\quad (3.50)$$

For $\alpha \rightarrow \pm \infty$ the parameter σ becomes independent of α

$$\sigma \sim \frac{\beta_{\infty} V_{\infty}^2 - \beta_{\infty} V^2}{\beta_{\infty} V_{\infty}^2 + \beta_{\infty} V^2} \quad \text{for } |\alpha| \sim \infty \quad (3.51)$$

and

$$\Sigma \sim \sigma e^{-2\beta_{\infty} |\alpha|} \quad (3.52)$$

We also remark that for the steady-state case the expression (3.51) is valid for all α .

The function Σ is real for $\alpha > \alpha_1^{\infty}$ or $\alpha < \alpha_2$. It is bounded uniformly on the real axis and never exceeds unity in absolute value (see Fig. 4). In the steady state it is bounded by σ . For low Mach number, we have approximately

$$\sigma \approx \frac{1 - V^2/V_{\infty}^2}{1 + V^2/V_{\infty}^2} \quad (3.53)$$

and

$$\frac{\delta^*}{\delta} = 1 - \frac{V}{V_{\infty}} = \frac{1}{N+1} \quad (3.54)$$

where δ^* is the displacement thickness and N is the index of a power law velocity profile. Thus

$$\frac{V}{V_{\infty}} = 1 - \frac{1}{N+1} = \frac{N}{N+1} \quad (3.55)$$

and

$$\begin{aligned}\sigma &= \frac{2N+1}{2N^2+2N+1} \\ &\approx .13 \quad \text{for } N = 7\end{aligned}\quad (3.56)$$

$$\Sigma = \sigma(a) e^{-2\Gamma a}$$

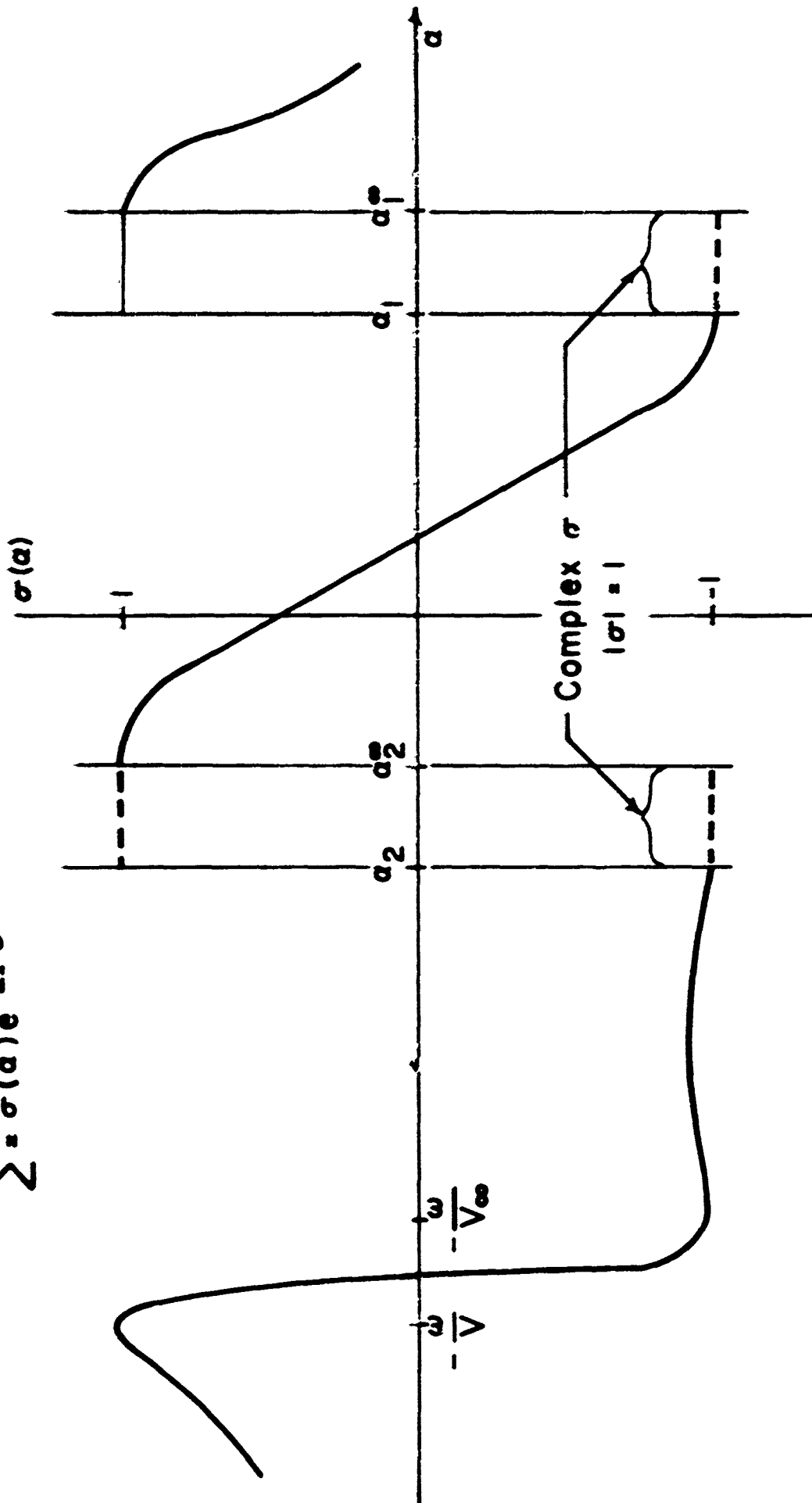


Fig. 4. Sketch of Complex σ Function on the Real Axis (see Eqs. (3.50) through (3.52)).

For a steady-state deflection σ is of the order of the boundary layer velocity defect, and we expect the iteration scheme to work. A rigorous proof could be developed.

Since Σ is only bounded by unity in the unsteady case, we can not prove a priori that the iteration scheme will work. However, it seems plausible that it will, at least for sufficiently low frequency. The question is whether we can ultimately calculate results for large enough frequency to see any significant nonsteady behavior near the trailing edge. We remark finally that when $\Sigma = 1$, the two-step shear layer has unstable eigensolutions and when $\Sigma = -1$, the wake has unstable eigensolutions. This fact may present some complications in obtaining a unique solution of the unsteady lifting surface problem. Further analysis of this important point should be carried out before we embark on a numerical solution of the unsteady problem.

IV. APPLICATIONS

We illustrate the foregoing theory with two examples. First, we calculate the lowest-order solution for the linear flap at zero frequency. Second, we consider an oscillating exponential flap for which we calculate lowest- and first-order results.

The Steady State Linear Flap

Consider the steady state deflected flap shown in Fig. 5. The surface deflection is given by

$$f(x) = -\phi(x - x_h)H(x - x_h) \quad (4.1)$$

where $H(x)$ is the Heaviside step function. The downwash and surface acceleration are

$$W = Vf' = -\phi VH(x - x_h) \quad (4.2)$$

and

$$\frac{DW}{Dx} = VW' = -\phi V^2 \delta(x - x_h) \quad (4.3)$$

where $\delta(x)$ is the Dirac delta function. It is understood that x is negative in all of the subsequent formulas.

The lowest-order surface pressure is obtained with (3.31). We have

$$\begin{aligned} p_o(x) &= \frac{1}{\beta\theta} \int_x^0 N_1(s-x) ds \int_0^\infty N_2(\xi) \left[\frac{DW}{D\eta} \right]_{s-\xi} d\xi \\ &= -\frac{\phi V^2}{\beta\theta} \int_x^0 N_1(s-x) ds \int_0^\infty N_2(\xi) \delta(s-\xi-x_h) d\xi \\ &= -\frac{\phi V^2}{\beta\theta} \int_{\text{Max}(x, x_h)}^0 N_1(s-x) N_2(s-x_h) ds \\ &= -\frac{\phi V^2}{\pi\beta\theta} \int_{\text{Max}(x, x_h)}^0 \frac{1}{\sqrt{s-x} \sqrt{s-x_h}} ds \\ &= -\frac{2\phi V^2}{\pi\beta\theta} \ln \left[\frac{(-x)^{1/2} + (-x_h)^{1/2}}{|x-x_h|^{1/2}} \right] \end{aligned} \quad (4.4)$$

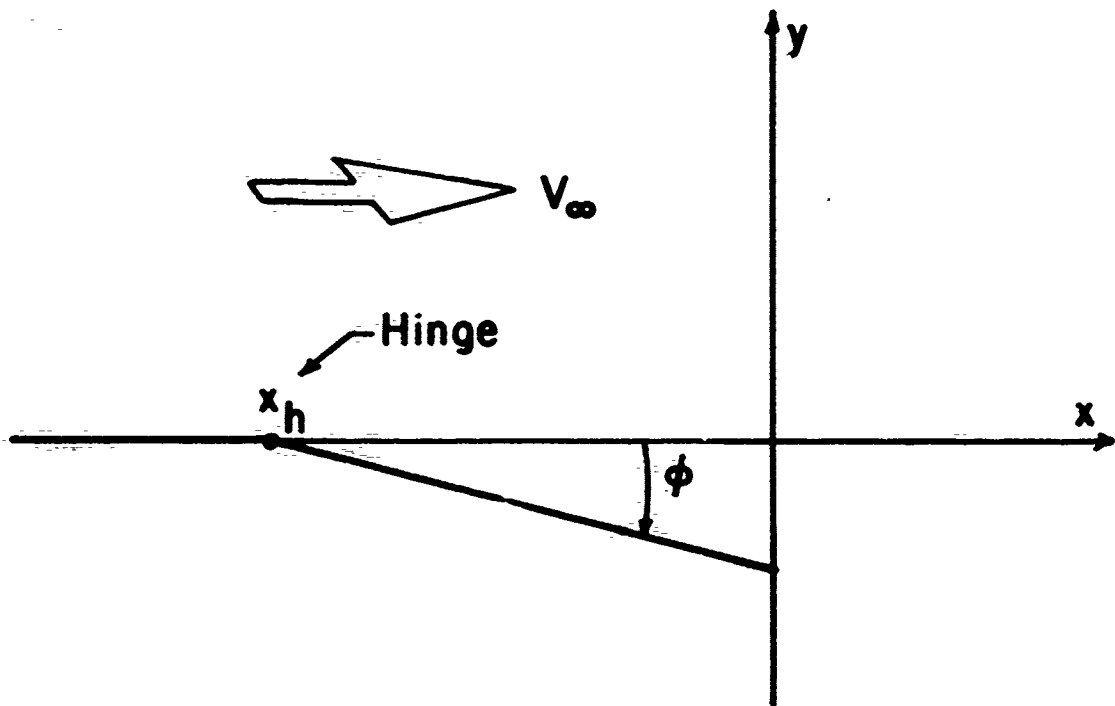


Fig. 5. The Linear Flap

With $\beta = \beta_\infty$ and $\theta = 1$ the last result is the exact solution of the linear deflected flap in a nonshear flow. The pressure is plotted in Fig. 6.

Remarks

We note several asymptotic results. First, the pressure tends to zero as $(x/x_h)^{1/2}$ at the trailing edge and has a logarithmic singularity at the hinge line in accordance with known results for the finite airfoil (see Ref. 13, e.g.). Also, the pressure tends to zero as $(x_h/x)^{1/2}$ for $x \rightarrow -\infty$. This means that the total lift on the plate is noncalculable. In fact, the lift on any length L of the trailing edge tends to infinity as \sqrt{L} for $L \rightarrow \infty$. This is in agreement with the known exact solution (Ref. 14) for the lift on a finite airfoil with chord c at zero angle of attack, but with a finite flap deflection. The total lift tends to infinity as \sqrt{c} . We shall discuss the implication of this singular result in more detail after we consider the next example.

The Exponential Flap (Zero Order)

The linear flap is a simple example of the lowest-order steady state solution. However, the algebra becomes very tedious when higher-order or even unsteady results are sought. For this reason, we consider the unsteady exponential flap illustrated in Fig. 7. The flap deflection mode is assumed to be exponential; i.e.,

$$\hat{f}(x) = -\phi e^{x/\ell} \quad (4.5)$$

so that

$$W = \frac{Df}{Dx} = -\alpha V(1 - ik)e^{x/\ell} \quad (4.6)$$

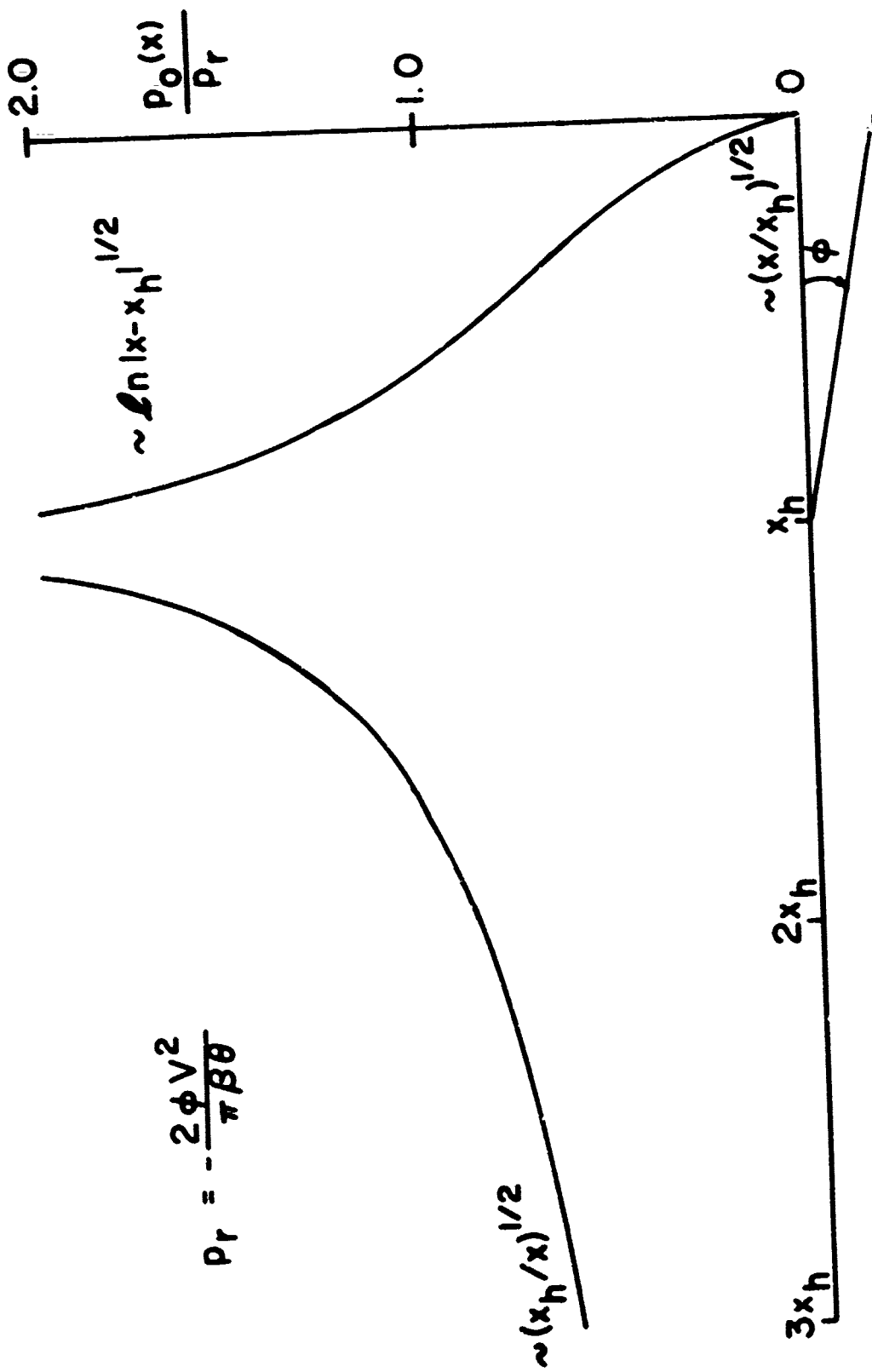
and

$$\frac{DW}{Dx} = -\frac{\phi}{\ell}(1 - ik)^2 e^{x/\ell} \quad (4.7)$$

where

$$k = \omega\ell/V, \text{ reduced frequency}$$

and ϕ is an effective flap angle; i.e. $\phi = -f'(0)$.



$$p_r = -\frac{2\phi V^2}{\pi \beta \theta}$$

Fig. 6. Pressure Distribution on the Linear Flap

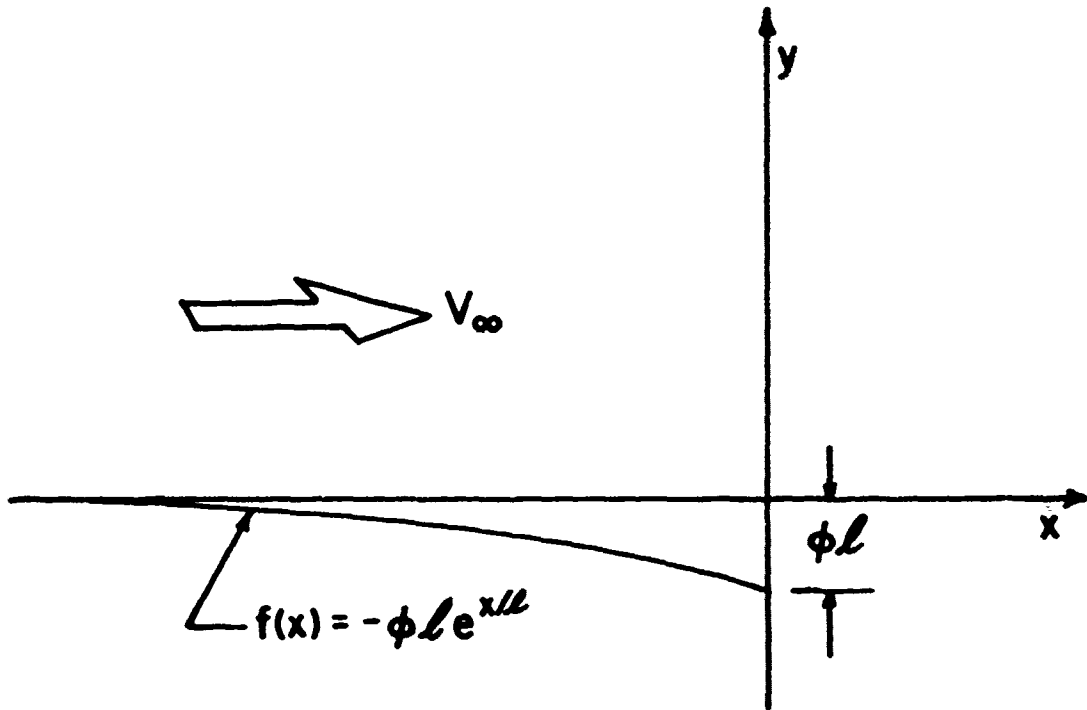


Fig. 7. The Exponential Flap

Our next step is to calculate the function $Q_0^*(x)$ with (3.29) and $Q_0(\alpha)$ with (3.26). We have

$$Q_0^*(x) = \frac{1}{\beta\theta} \int_0^{\infty} N_2(\xi) \left[\frac{DW}{D\eta} \right]_{x-\xi} d\xi$$

$$= - \frac{\phi V^2 (1-ik)^2}{\beta\theta l} e^{x/l} \int_0^{\infty} e^{-\xi/l} N_2(\xi) d\xi \quad (4.8)$$

With $N_2(x)$ given by (3.21), we get

$$\int_0^{\infty} e^{-\xi/l} N_2(\xi) d\xi = \int_0^{\infty} e^{-\xi/l} \frac{e^{-i\alpha_2 \xi - i\pi/4}}{\sqrt{\pi \xi}} d\xi = \frac{l^{1/2} e^{-i\pi/4}}{(1 + i\alpha_2 l)^{1/2}} \quad (4.9)$$

so that

$$Q_0^*(x) = (2\pi)^{1/2} \frac{C}{l} e^{x/l} \quad (4.10)$$

where

$$C = - \frac{\phi V^2 (1-ik)^2 l^{1/2} e^{-i\pi/4}}{\beta\theta (1+i\alpha_2 l)^{1/2} (2\pi)^{1/2}} \quad (4.11)$$

The complex function $Q_0(\alpha)$ follows from (3.26):

$$Q_0(\alpha) = \frac{1}{(2\pi)^{1/2}} \int_{-\infty}^0 e^{i\alpha x} Q_0^*(x) dx$$

$$= \frac{C}{l} \int_{-\infty}^0 e^{i\alpha x} e^{x/l} dx$$

$$= \frac{C}{1 + i\alpha l} \quad (4.12)$$

Thus, $Q_0(\alpha)$ is a simple pole at $\alpha = 1/l$.

The lowest order pressure follows from (3.28). We get

$$\begin{aligned}
p_0(x) &= \int_x^0 N_1(\xi - x) Q_0^*(\xi) d\xi \\
&= C \sqrt{\frac{2}{\ell}} e^{i\pi/4} \cdot e^{x/\ell} \int_0^{-x/\ell} e^{(1+i\alpha_1\ell)s} \frac{ds}{\sqrt{s}} \quad (4.13)
\end{aligned}$$

The integral in (4.13) can be expressed in several different forms with the complex error function. However, the simplest form for computational purposes is to write the real and imaginary parts out separately. Thus, we get after substituting for C :

$$p_0(x) = -\frac{\phi V^2}{\beta \theta} \frac{(1 - ik)^2}{(1 + i\alpha_2\ell)^{1/2}} \sqrt{\frac{2}{\pi}} G\left[(-x/\ell)^{1/2}\right] \quad (4.14)$$

where

$$G(z) = e^{-z^2} \int_0^z e^{(1+i\alpha_1\ell)t^2} dt \quad (4.15)$$

and

$$\begin{aligned}
\operatorname{Re}G(z) &= e^{-z^2} \int_0^z e^{t^2} \cos(\alpha_1\ell t^2) dt \\
\operatorname{Im}G(z) &= e^{-z^2} \int_0^z e^{t^2} \sin(\alpha_1\ell t^2) dt \quad (4.16)
\end{aligned}$$

The oscillating exponential flap can thus be solved completely in lowest order and expressed in terms of simple functions.

It is interesting to consider the steady state exponential flap. We have

$$p_0(x) = -\frac{\phi V^2}{\beta \theta} \sqrt{\frac{2}{\pi}} F\left[(-x/\ell)^{1/2}\right] \quad (4.17)$$

where

$$F(z) = e^{-z^2} \int_0^z e^{t^2} dt \quad (4.18)$$

is Dawson's integral (see Ref. 15). The pressure profile corresponding to (4.18) is plotted in Fig. 8. The pressure tends to zero

$$Pr = -\frac{2\phi V^2}{\pi\beta\theta}$$

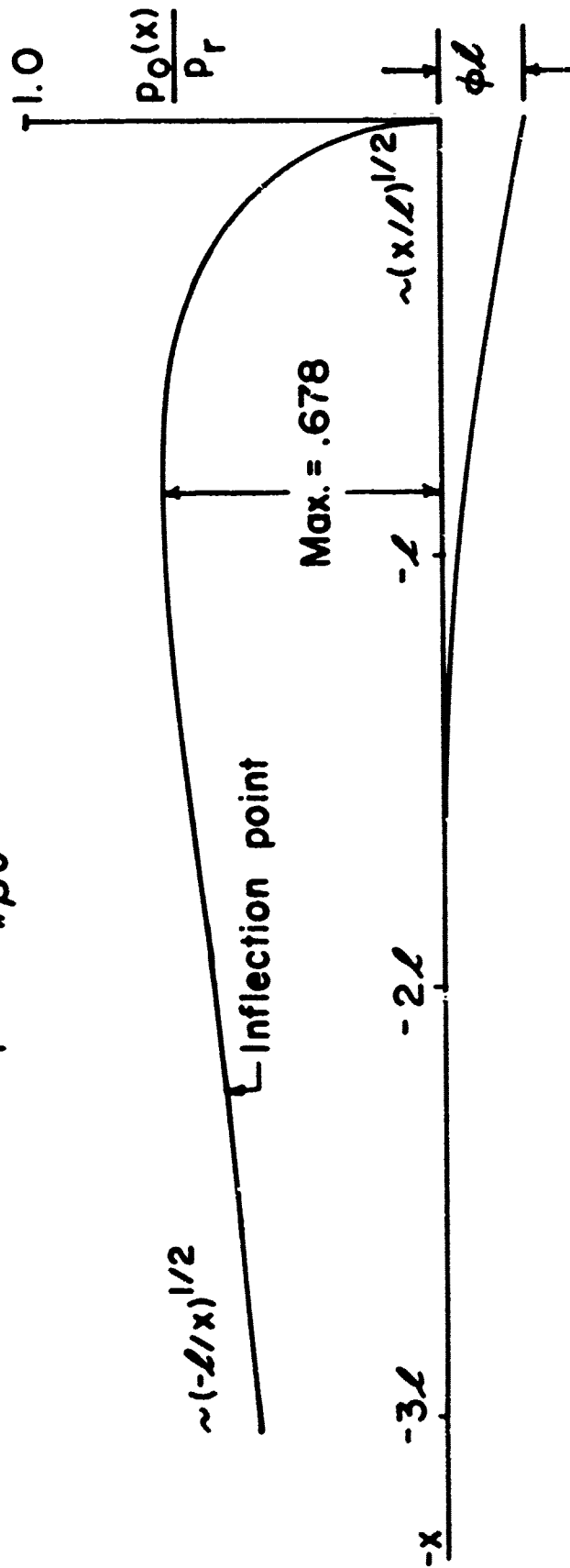


Fig. 8. Pressure Distribution on the Exponential Flap

as $\sqrt{-x/l}$ as $x \rightarrow 0^-$, and tends to zero as $\sqrt{-l/x}$ for $x \rightarrow -\infty$. Thus, the total lift is again infinite, a result that does not seem to depend upon the details of the surface deflection. The pressure has a minimum as indicated in Fig. 8. Thus

$$|\text{Min } p_0| = .541 \sqrt{\frac{2}{\pi}} \frac{\rho V^2}{\beta \theta}$$

at

$$\frac{x}{l} = - .8541 \quad (4.19)$$

First-Order Exponential Flap (Steady State)

Because of the simplicity of the function $Q_0(\alpha)$, we can derive first-order results for the exponential flap in steady state. In principal, the unsteady first-order result can be calculated but the details are extremely tedious. The pertinent formulas of Section III are summarized below:

$$\begin{aligned} p_1(x) &= p_0(x) + p'(x) \\ p'(x) &= \int_x^0 P^-(\xi) N_1(\xi - x) d\xi \\ P^-(x) &= \frac{2}{(2\pi)^{1/2}} \int_{-\infty}^0 Q_0^*(\xi) \Sigma^*(x - \xi) d\xi \\ \Sigma^*(x) &= \frac{1}{(2\pi)^{1/2}} \int_{-\infty}^{\infty} e^{-i\alpha x} \Sigma(\alpha) d\alpha \end{aligned} \quad (4.20)$$

where

$$\Sigma(\alpha) = \sigma e^{-2\beta\delta|\alpha|}, \quad \omega = 0 \quad (4.21)$$

and

$$\sigma = \frac{\beta \theta V_\infty^2 - \beta_\infty V^2}{\beta \theta V_\infty^2 + \beta_\infty V^2}, \quad \omega = 0 \quad (4.22)$$

Again, it is understood that $x < 0$ in all of the formulas (4.20).

The reason for the simplicity of the steady state case is that σ , defined by (4.22), is independent of α . Thus, we can evaluate each of the functions needed in the series of convolution integrals in (4.20). First, we calculate

$$\begin{aligned} \Sigma^*(x) &= \frac{\sigma}{(2\pi)^{1/2}} \int_{-\infty}^{\infty} e^{-i\alpha x} e^{-2\beta\delta\|\alpha\|} d\alpha \\ &= \frac{2\sigma}{(2\pi)^{1/2}} \int_0^{\infty} e^{-2\beta\delta\alpha} \cos \alpha x \\ &= \frac{1}{(2\pi)^{1/2}} \frac{4\sigma\beta\delta}{x^2 + 4\beta^2\delta^2} \end{aligned} \quad (4.23)$$

We substitute this result together with (4.10) into the third formula of (4.20) to obtain

$$\begin{aligned} P^*(x) &= \frac{8C\sigma\beta\delta}{(2\pi)^{1/2} \cdot l} \int_{-\infty}^0 \frac{e^{\xi/l} d\xi}{(x-\xi)^2 + 4\beta^2\delta^2} \\ &= \frac{8C\sigma\beta\delta}{(2\pi)^{1/2} \cdot l^2} e^{x/l} \int_{x/l}^{\infty} \frac{e^{-s} ds}{s^2 + 4\beta^2\delta^2/l^2} \end{aligned} \quad (4.24)$$

The last result can be expressed in terms of exponential integrals, but it is more convenient to leave it in the simple integral form for the moment.

Finally, we substitute (4.24) together with the definition of N_1 (see (3.21)) into the expression for $p^*(x)$. We get

$$\begin{aligned} p^*(x) &= \int_x^0 P^*(\xi) N_1(\xi - x) d\xi \\ &= \frac{8C\sigma\beta\delta}{(2\pi)^{1/2} l^2 \sqrt{\pi}} \int_x^0 \frac{e^{\xi/l} d\xi}{(\xi - x)^{1/2}} \int_{\xi/l}^{\infty} \frac{e^{-s} ds}{s^2 + 4\beta^2\delta^2/l^2} \end{aligned} \quad (4.25)$$

or after some manipulation of the double integral

$$p'(x) = -\frac{\phi V^2}{3\theta} \sqrt{\frac{2}{\pi}} 2\sigma F\left[\left(-\frac{x}{l}\right)^{1/2}, \frac{2\beta\delta}{l}\right] \quad (4.26)$$

where

$$F(z, \epsilon) = e^{-z^2} \int_0^z e^{t^2} dt \cdot \frac{\epsilon}{\pi} \int_{t^2-z^2}^{\infty} \frac{e^{-s} ds}{s^2 + \epsilon^2} \quad (4.27)$$

The final expression for the first-order pressure is

$$p_1(x) = -\frac{2\phi V^2}{\sqrt{\pi} l \beta \theta} \left\{ F\left[\left(-\frac{x}{l}\right)^{1/2}\right] + 2\sigma F\left[\left(-\frac{x}{l}\right)^{1/2}, \frac{2\beta\delta}{l}\right] \right\} \quad (4.28)$$

The function $F(z, \epsilon)$ is a generalization of Dawson's integral; i.e.,

$$\lim_{\epsilon \rightarrow 0} F(z, \epsilon) = F(z) \quad (4.29)$$

where $F(z)$ is given by (4.18). Thus we can also write (4.28) in the form

$$p_1(x) = -\frac{2\phi V^2}{\sqrt{\pi} \beta \theta} \left\{ (1 + 2\sigma) F\left[\left(-\frac{x}{l}\right)^{1/2}\right] - 2\sigma F^*\left[\left(-\frac{x}{l}\right)^{1/2}, \frac{2\beta\delta}{l}\right] \right\} \quad (4.30)$$

where

$$F^*(z, \epsilon) = e^{-z^2} \int_0^z e^{t^2} dt \cdot \frac{\epsilon}{\pi} \int_{t^2-z^2}^{\infty} \frac{1 - e^{-s}}{s^2 + \epsilon^2} ds \quad (4.31)$$

Asymptotic Results

There are two independent parameters in our first-order shear layer result. The basic expansion parameter is σ and terms of order σ^2 have been neglected. This parameter is truly a property of the shear layer as we have shown in Section III (see (3.53) to (3.56)). The second parameter is $2\beta\delta/l$ and it is the ratio of the shear layer thickness to the length scale of the flap. We can vary

this parameter independently of σ . For example, when $\delta/l \rightarrow 0$ the pressure is given by the first term in (4.30); i.e.,

$$\lim_{\delta/l \rightarrow 0} p_1(x) = - \frac{2\phi V^2}{\sqrt{\pi} \beta \theta} (1 + 2\sigma) F\left[\left(-\frac{x}{l}\right)^{1/2}\right] \quad (4.32)$$

In the complete absence of a shear layer, we have

$$p_0(x) = - \frac{2\phi V_\infty^2}{\sqrt{\pi} \beta_\infty} F\left[\left(-\frac{x}{l}\right)^{1/2}\right] \quad (4.33)$$

so that

$$\bar{\gamma} \equiv \frac{p_1(x)}{p_0(x)} = \frac{\beta_\infty}{\beta \theta} \frac{V^2}{V_\infty^2} (1 + 2\sigma) \quad (4.34)$$

The importance of the factor 2σ is now clear. Without this term (4.32) would tell us that the lowest-order pressure is to be obtained by replacing the entire flow by a uniform flow with the velocity and temperature (or density) of the shear layer. This is a gross over-correction of the inviscid result and must not be used. The correct factor to use is $\bar{\gamma}$ given by (4.34).

For low Mach number $M_\infty^2 \ll 1$ we can express γ in terms of the shear layer velocity defect; i.e.,

$$\Delta = \frac{\delta^*}{\delta} = 1 - \frac{V}{V_\infty} \quad (4.35)$$

Then

$$\begin{aligned} \gamma &\equiv \frac{V^2}{V_\infty^2} \left[1 + 2 \left(\frac{V_\infty^2 - V^2}{V_\infty^2 + V^2} \right) \right] \\ &= (1 - \Delta)^2 \left[1 + \frac{\Delta(2 - \Delta)}{1 - \Delta + \Delta^2/2} \right] \\ &= [1 - 2\Delta + O(\Delta^2)][1 + 2\Delta + O(\Delta^2)] \\ &= 1 - O(\Delta^2) \end{aligned} \quad (4.36)$$

The correction due to the shear layer is $O(\Delta^2)$ and is therefore noncalculable with first-order theory when $\delta/l \rightarrow 0$.

For $\delta/l = 0(1)$ we must in general use (4.30) to calculate the shear layer correction. For small δ/l we can estimate the order of the correction with the asymptotic results derived in Appendix B. We have

$$F^*(\sqrt{z}, \epsilon) = \frac{1}{2} \int_0^z \frac{e^{-\eta} G(\eta, \epsilon)}{\sqrt{z-\eta}} d\eta \quad (4.37)$$

$$\begin{aligned} G(\eta, \epsilon) &= \frac{\epsilon}{\pi} \int_{-\eta}^{\infty} \frac{1 - e^{-s}}{s^2 + \epsilon^2} ds \\ &= 1 - \frac{1}{\pi} \tan^{-1} \frac{\epsilon}{\eta} \\ &\quad - \frac{1}{2\pi i} \left[e^{-i\epsilon} E_1(-\eta - i\epsilon) - e^{i\epsilon} E_1(-\eta + i\epsilon) \right] \end{aligned} \quad (4.38)$$

where

$$E_1(z) = \int_z^{\infty} \frac{e^{-t}}{t} dt \quad |\arg z| < \pi \quad (4.39)$$

For $\epsilon \rightarrow 0$ we have further

$$F^*(\sqrt{z}, \epsilon) \underset{G \rightarrow 0}{=} \frac{\epsilon}{2\pi} \int_0^z \frac{d\eta}{\sqrt{z-\eta}} \left\{ e^{-\eta} \left[\ln \frac{\eta}{(\eta^2 + \epsilon^2)^{1/2}} - E_1(\eta) \right] + \frac{1 - e^{-\eta}}{\eta} \right\} \quad (4.40)$$

where

$$E_1(\eta) = - \int_{\eta}^{\infty} \frac{e^{-t}}{t} dt \quad (4.41)$$

In the vicinity of the trailing edge, we get

$$F^*(\sqrt{z}, \epsilon) \underset{\substack{\epsilon \rightarrow 0 \\ z \rightarrow 0}}{\approx} \frac{\epsilon}{\pi} \left(\ln \frac{1}{\epsilon} + 1 - \gamma \right) \sqrt{z} \quad (4.42)$$

where $\gamma = .57721$ is Euler's constant. Thus, the first-order pressure tends to zero as $\sqrt{-x}$ near the trailing edge. However,

the magnitude of the correction is $O(\epsilon \ln 1/\epsilon)$ where $\epsilon = 2\beta\delta/l$. We conclude that any expansion of the shear layer solution in powers of ϵ must fail in the vicinity of the trailing edge.

For large z it is also shown in Appendix B that $F^*(\sqrt{z}, \epsilon)$ decays like $(1/z^{3/2})$. Thus, the pressure at large distances from the trailing edge is given by the lowest-order result with the multiplicative correction discussed above (see (4.32)).

The Paradox of Infinite Lift - A Suggested Experiment

We have seen that in the absence of a shear layer the total lift on any section of the trailing edge of length L grows as \sqrt{L} . This result is in complete agreement with the exact solution for a finite length flapped airfoil (see Ref. 14, e.g.). One can argue that in reality this result cannot be true. The total lift must either reach a maximum or decay as the airfoil chord is increased without bound for fixed flap geometry. The flap eventually becomes totally immersed in the shear layer and must become totally ineffective in producing lift. Thus, the "steady flapped airfoil" offers a means for investigating the role of a shear layer in limiting the lift.

The paradox could perhaps be resolved with a very simple experiment. A two-dimensional flat plate airfoil could be fitted with a flap of fixed chord. The chord of the airfoil section forward of the flap could be varied while the total steady state lift is measured. A plot of $\ln(\text{Lift})$ versus $\ln(c/l)$ would be expected to appear something like that shown in Fig. 9. The ratio c/l where the lift starts to depart from the no-shear result (straight line with slope 1/2 in Fig. 9) would be a measure of the critical ratio of shear layer thickness to flap chord. With more detailed theory, this point could also be calculated. The two-step model does not appear to have the potential for describing the saturation because the velocity at the surface of the airfoil cannot be reduced below a fixed value as the shear layer thickness is

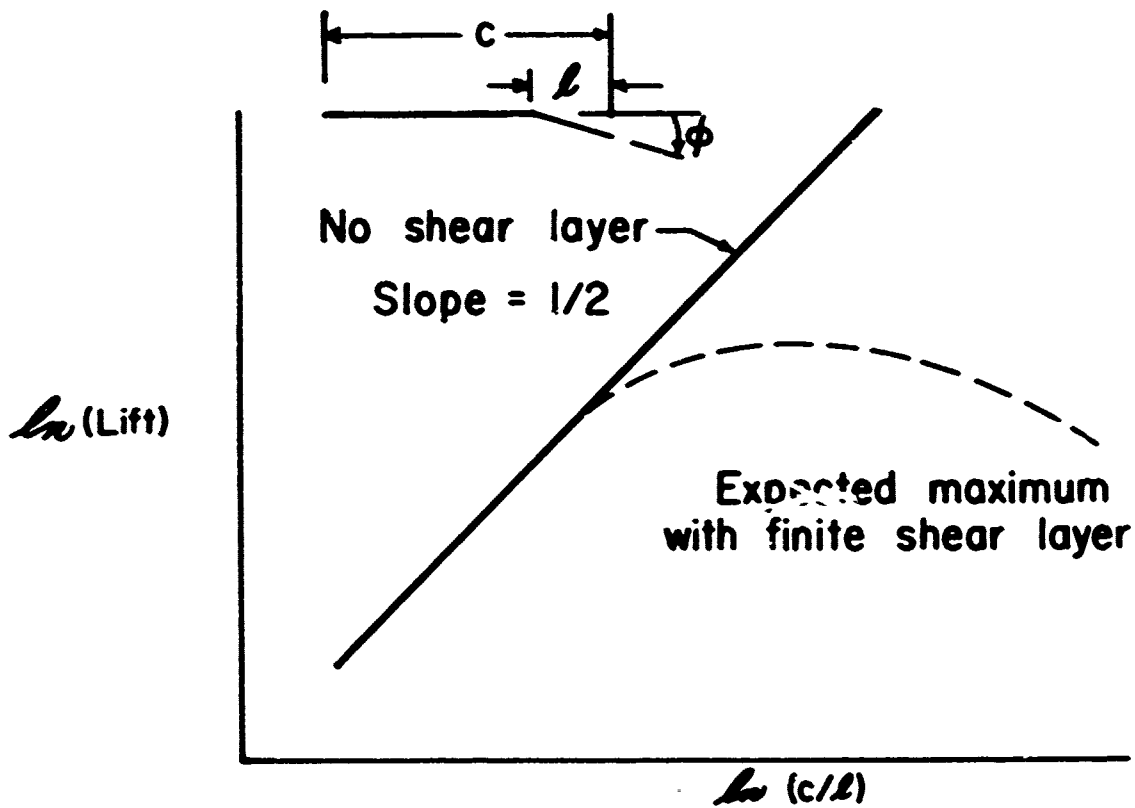


Fig. 9. Suggested Airfoil Experiment

increased. A linear velocity profile or a power law profile would be more realistic, although the Wiener-Hopf analysis may become intractable.

The Unsteady Trailing Edge

To continue the investigation of the shear layer effect on the unsteady trailing edge lift, it would be desirable to carry out the first-order analysis for the two-layer model. The essential and nontrivial step in the analysis is to calculate the inverse Fourier transform of the shear layer function $\Sigma(\alpha)$ given by (3.8) and (3.9). Given $\Sigma^*(x)$ the first-order pressure is a matter of integration (see (3.35) through (3.38)). These results would be of immense value in assessing the role of the shear layer on the unsteady lift.

V. CONCLUSIONS

We have investigated the problem of an oscillating trailing edge that is immersed in a two-dimensional subsonic shear flow. The ideal problem wherein the shear layer is replaced by a two-step model is given detailed consideration. An approximate solution is developed to first order in the shear layer velocity defect (ratio of displacement thickness to boundary layer thickness) and is valid for arbitrary length scale of the trailing edge deflection.

The general solution is applied to calculate the steady state lift on a linearly deflected flap and the unsteady lift on an exponential flap. The latter example is developed to first order for the steady state. The principle conclusions of our analysis are as follows:

1. The lowest-order steady state lift distribution tends to zero as the square root of the distance from the trailing edge for small distance and as the reciprocal square root of the distance for large distance. The linear flap has a weak logarithmic singularity in lift at the hinge line in accordance with known results.
2. The total lift on a trailing edge section of length L becomes infinite like \sqrt{L} as L is increased without bound. This result is in agreement with the thin airfoil solution for a finite length flapped airfoil.
3. The first-order lift on the steady exponential flap is developed in detail. It is shown that the trailing edge pressure correction varies as $\sqrt{|x|}$ and is attenuated by a term of $O(\epsilon \ln 1/\epsilon)$ where $\epsilon = \delta^*/l$ is the ratio of shear layer thickness to flap length. We conclude that any attempt to expand the solution of the trailing edge problem in a regular perturbation series must fail near the trailing edge.

REFERENCES

1. Yates, John E.: Linearized Integral Theory of Three-Dimensional Unsteady Flow in a Shear Layer, AIAA Journal, Vol. 12, No. 5, May 1974, pp. 596-602.
2. Yates, John E.: Linearized Integral Theory of the Viscous Compressible Flow Past a Wavy Wall, AFOSR-TR-1335, July 1972, Aeronautical Research Associates of Princeton, Princeton, New Jersey.
3. Yates, John E.: Linearized Integral Theory of Three-Dimensional Unsteady Compressible Flow in a Shear Layer Bounded by an Oscillating Wall, AFOSR-TR-73-1123, June 1973.
4. Yates, John E.: LaPlace Transform Theory of Supersonic Panel Flutter Including Boundary Layer Effects, A.R.A.P. Report No. 250, December 1975.
5. Yates, John E.: ZYNAPF - Zeydel Yates NASA Air Force Panel Flutter, A.R.A.P. Report No. 249, December 1975.
6. Yates, John E. and Sandri, Guido: Bernoulli Enthalpy: A Fundamental Concept in the Theory of Sound, AIAA Paper 75-439, March 24-26, 1975.
7. Yates, John E. and Sandri, Guido: The Role of Bernoulli Enthalpy in the Scattering of Sound, AIAA Paper No. 76-5, January 26-28, 1976.
8. Dowell, E.H. and Ventres, C.S.: Derivation of Aerodynamic Kernel Functions, AIAA Journal, Vol. 11, No. 11, Nov. 1973, pp. 1586-1588.
9. Ventres, C.S.: Nonsteady Shear Flow Lifting Surface Theory, BBN Report No. 3235, Bolt Beranek and Newman, Inc., Boston, Mass., January 30, 1976. Also see: Shear Flow Aerodynamics: Lifting Surface Theory, AIAA J., Vol. 13, No. 9, September 1975.
10. Williams, M.H.: The Resolvent of Singular Integral Equations, Princeton University, Princeton, N.J.
11. Dowell and Chi: Private communication of April 8, 1976.
12. Noble, B.: Methods Based on the Wiener-Hopf Technique, Pergamon Press: New York, 1958.
13. Goldstein, Marvin E.: Boundary-Layer Effect in Panel Flutter, AIAA Journal, Vol. 13, No. 9, September 1975.
14. von Karman, Th. and Burgers, J.M.: General Aerodynamic Theory-Perfect Fluids, in Aerodynamic Theory, Vol. II, Div. E (Wm. F. Durand, ed.), Calif. Institute of Tech., Calif., January 1943, p. 56.
15. Abramowitz, M. and Stegun, I.A., eds., Handbook of Mathematical Functions (2nd printing), National Bureau of Standards, Washington, D.C., 1964.

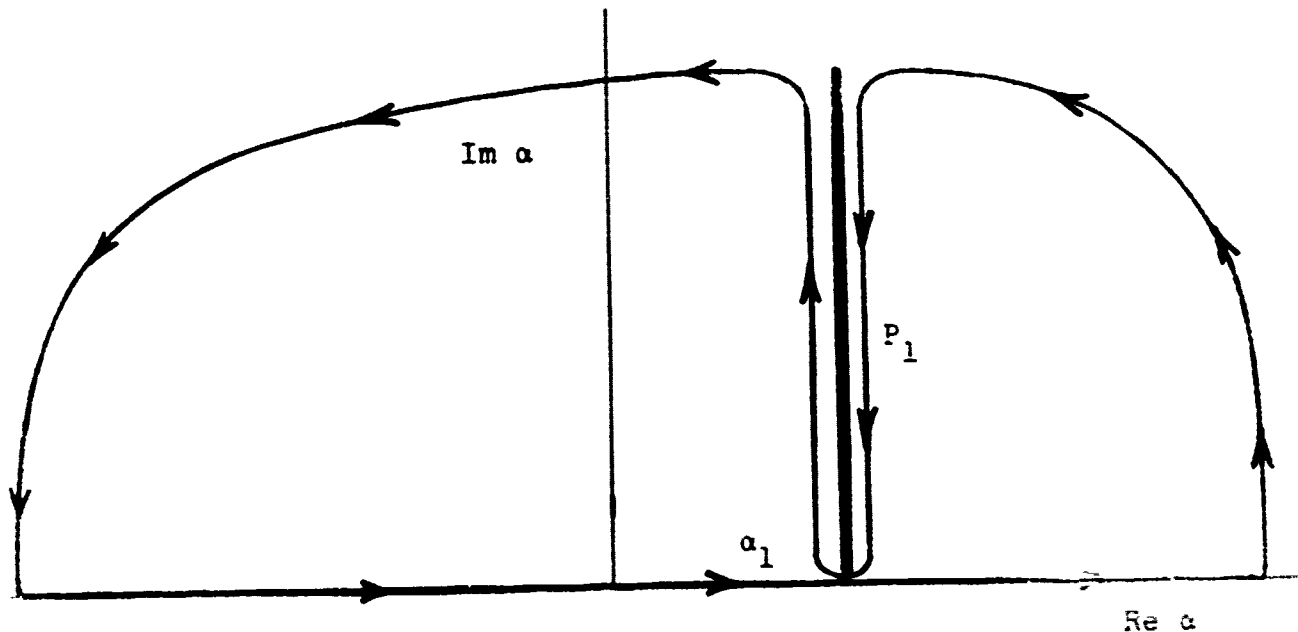
APPENDIX A

EVALUATION OF $N_1(x)$ AND $N_2(x)$

Consider the integral definition of $N_1(x)$; i.e.,

$$\int_0^{\infty} e^{-i\alpha\xi} N_1(\xi) d\xi = \frac{1}{(\alpha - \alpha_1)^{1/2}} \quad (\text{A.1})$$

where the complex function $(\alpha - \alpha_1)^{1/2}$ is defined by the branch cut shown in the following sketch:



Multiply (A.1) by $e^{i\alpha x}$ and integrate over all α to get

$$N_1(x) = \frac{1}{2\pi} \int_{-\infty}^{\infty} \frac{e^{i\alpha x}}{(\alpha - \alpha_1)^{1/2}} d\alpha \quad (\text{A.2})$$

Since $(\alpha - \alpha_1)^{1/2}$ is analytic in the lower half plane, the function $N_1(x)$ is zero for negative x . For $x > 0$ we use the contour shown in the above sketch to evaluate the integral.

We have

$$N_1(x) = -\frac{1}{\pi} \int_{P_1}^{\alpha_1} \frac{e^{i\alpha x} d\alpha}{(\alpha - \alpha_1)^{1/2}} \quad (\text{A.3})$$

Let

$$\alpha = \alpha_1 + \frac{t^2 e^{i\pi/2}}{x} \quad (\text{A.4})$$

Then

$$\begin{aligned} N_1(x) &= \frac{2}{\pi} \frac{e^{i\alpha_1 x + i\pi/4}}{\sqrt{x}} \int_0^{\infty} e^{-t^2} dt \\ &= \frac{e^{i\alpha_1 x + i\pi/4}}{\sqrt{\pi x}} \quad x > 0 \end{aligned} \quad (\text{A.5})$$

The evaluation of $N_2(x)$ is similar to $N_1(x)$ except that the contour in the complex α plane must be closed around the branch cut from α_2 into the lower-half plane. We get

$$\begin{aligned} N_2(x) &= \frac{1}{2\pi} \int_{-\infty}^{\infty} \frac{e^{-i\alpha x}}{(\alpha - \alpha_2)^{1/2}} d\alpha \\ &= \frac{e^{-i\alpha_2 x - i\pi/4}}{\sqrt{\pi x}}, \quad x > 0 \\ &= 0, \quad x < 0 \end{aligned} \quad (\text{A.6})$$

APPENDIX B
ASYMPTOTIC ANALYSIS OF $F^*(z, \epsilon)$

Consider the function

$$F^*(\sqrt{z}, \epsilon) = \frac{1}{2} \int_0^z \frac{e^{-\eta} G(\eta, \epsilon)}{\sqrt{z-\eta}} d\eta \quad (B.1)$$

with

$$G(\eta, \epsilon) = \frac{\epsilon}{\pi} \int_{-\eta}^{\infty} \frac{1 - e^{-s}}{s^2 + \epsilon^2} ds \quad (B.2)$$

In general, F^* must be evaluated numerically. We consider below the asymptotic behavior as $\epsilon \rightarrow 0$ with $z = 0(1)$. First, we evaluate $G(\eta, \epsilon)$ in terms of known functions. We have

$$G(\eta, \epsilon) = G_0(\eta, \epsilon) - G_1(\eta, \epsilon) \quad (B.3)$$

where

$$G_0(\eta, \epsilon) = \frac{\epsilon}{\pi} \int_{-\eta}^{\infty} \frac{ds}{s^2 + \epsilon^2} \quad (B.4)$$

$$G_1(\eta, \epsilon) = \frac{\epsilon}{\pi} \int_{-\eta}^{\infty} \frac{e^{-s} ds}{s^2 + \epsilon^2} \quad (B.5)$$

The first integral is easily evaluated in terms of the arc tangent. We get

$$G_0(\eta, \epsilon) = 1 - \frac{1}{\pi} \tan^{-1} \frac{\epsilon}{\eta} \quad (B.6)$$

To evaluate the second integral we expand the integrand by partial fractions and translate the dummy variable of integration in each part. We get

$$\begin{aligned}
G_1(\eta, \epsilon) &= \frac{1}{2\pi i} \int_{-\eta}^{\infty} e^{-s} \left(\frac{1}{s-1} - \frac{1}{s+1} \right) ds \\
&= \frac{1}{2\pi i} \left(e^{-i\epsilon} \int_{-\eta-i\epsilon}^{\infty} \frac{e^{-t}}{t} dt - e^{i\epsilon} \int_{-\eta+i\epsilon}^{\infty} \frac{e^{-t}}{t} dt \right) \\
&= \frac{1}{2\pi i} \left[e^{-i\epsilon} E_1(-\eta - i\epsilon) - e^{i\epsilon} E_1(-\eta + i\epsilon) \right] \quad (B.7)
\end{aligned}$$

and

$$G(\eta, \epsilon) = 1 - \frac{1}{\eta} \tan^{-1} \frac{\epsilon}{\eta} - G_1(\eta, \epsilon) \quad (B.8)$$

where the exponential integral is defined by

$$E_1(z) = \int_z^{\infty} \frac{e^{-t}}{t} dt, \quad |\arg z| < \pi \quad (B.9)$$

To obtain the asymptotic expansion of F^* for small ϵ we must first develop a uniformly valid expansion of $G(\eta, \epsilon)$. We use the method of matched asymptotic expansion to accomplish this task. First, we expand $G(\eta, \epsilon)$ in the limit $\epsilon \rightarrow 0$ and $\eta = O(1)$. Then we expand G for $\epsilon \rightarrow 0$ and $\eta = O(\epsilon)$. The two expansions are then shown to have a common domain of validity by matching. Finally, we form an additive composite expansion with the two results.

Expand $G(\eta, \epsilon)$ for $\epsilon \rightarrow 0, \eta = O(1)$

We use known properties of the exponential integral to carry out the following program (see Ref. 15, p. 225). First, we expand E_1 as follows:

$$\begin{aligned}
E_1(-\eta \pm i\epsilon) &= \int_{-\eta \pm i\epsilon}^{-\eta \pm i0} \frac{e^{-t}}{t} dt + E_1(-\eta \pm i0) \\
&= \frac{1e^\eta}{\eta} \int_{i0}^{\pm\epsilon} \frac{e^{-1\tau}}{1 - i\tau/\eta} d\tau + E_1(-\eta \pm i0) \\
&= -E_1(\eta) \mp i\pi \pm i\epsilon \frac{e^\eta}{\eta} + O(\epsilon^2) \tag{B.10}
\end{aligned}$$

The last result is valid for all η greater than or equal $O(1)$. Now substitute the last result into (B.7) and combine the result with (B.9) to get

$$\begin{aligned}
\lim_{\substack{\epsilon \rightarrow 0 \\ \eta > O(1)}} G(\eta, \epsilon) &= -\frac{\epsilon}{\pi} \left[Ei(\eta) + \frac{1 - e^\eta}{\eta} \right] + O(\epsilon^2) \tag{B.11}
\end{aligned}$$

Expand $G(\eta, \epsilon)$ for $\epsilon \rightarrow 0$, $\eta = O(\epsilon)$

For η and ϵ both small we can write

$$E_1(-\eta \pm i\epsilon) = -\gamma - \ln(-\eta \pm i\epsilon) - \eta \pm i\epsilon + O(\epsilon^2) \tag{B.12}$$

where $\gamma = .57721$ is Euler's constant, and

$$\ln(-\eta \pm i\epsilon) = \ln(\eta^2 + \epsilon^2)^{1/2} \pm i\pi \pm i \tan^{-1} \frac{\epsilon}{\eta} \tag{B.13}$$

We use (B.12) and (B.13) in (B.7) and (B.8) to get

$$\begin{aligned}
\lim_{\substack{\epsilon \rightarrow 0 \\ \eta = O(\epsilon)}} G(\eta, \epsilon) &= -\frac{\epsilon}{\pi} \left[\ln(\eta^2 + \epsilon^2)^{1/2} + \gamma - 1 \right] + O(\epsilon^2) \tag{B.14}
\end{aligned}$$

which result is regular near $\eta = 0$ but is of $O(\epsilon \ln \epsilon)$.

Uniform Expansion of $G(\eta, \epsilon)$

Now we expand (B.11) for small η and (B.14) for large η . We get

$$\lim_{\eta \rightarrow 0} \left(\lim_{\substack{\epsilon \rightarrow 0 \\ \eta \geq 0(1)}} G(\eta, \epsilon) \right) = -\frac{\epsilon}{\pi} (\ln \eta + \gamma - 1) \quad (\text{B.15})$$

and

$$\lim_{\eta \rightarrow 0(1)} \left(\lim_{\substack{\epsilon \rightarrow 0 \\ \eta = 0(\epsilon)}} G(\eta, \epsilon) \right) = -\frac{\epsilon}{\pi} (\ln \eta + \gamma - 1) \quad (\text{B.16})$$

The last two results are identical so that the two asymptotic expansions have a common domain of validity. We form a uniformly valid composite expansion by adding (B.11) and (B.14) and subtracting the part they have in common (either (B.15) or (B.16)). The final result is

$$\lim_{\epsilon \rightarrow 0} G(\eta, \epsilon) = -\frac{\epsilon}{\pi} \left[E_1(\eta) + \frac{1 - e^{-\eta}}{\eta} - \ln \frac{\eta}{(\eta^2 + \epsilon^2)^{1/2}} \right] + O(\epsilon^2)$$

All η (B.17)

Finally, we substitute (B.17) into (B.1) to obtain

$$\lim_{\epsilon \rightarrow 0} F^*(\sqrt{z}, \epsilon) = +\frac{\epsilon}{2\pi} \int_C^z \frac{d\eta}{\sqrt{z-\eta}} \left\{ e^{-\eta} \left[\ln \frac{\eta}{(\eta^2 + \epsilon^2)^{1/2}} - E_1(\eta) \right] + \frac{1 - e^{-\eta}}{\eta} \right\} \quad (\text{B.18})$$

The last result is valid for all z and in general must be evaluated numerically. Unfortunately, the integral is not substantially more simple than the original integral (B.1) that is valid for arbitrary ϵ .

We conclude our analysis of F^* with results for small and large z . For $z \rightarrow 0$, we use the limit value of the expression in curly braces in (B.18). We get

$$F^*(\sqrt{z}, \epsilon) = \frac{\epsilon}{2\pi} \ln \left(\frac{z}{\epsilon} + 1 - \gamma \right) \int_C^z \frac{d\eta}{\sqrt{z-\eta}} = \frac{\epsilon}{\pi} \left(\ln \frac{1}{\epsilon} + 1 - \gamma \right) \sqrt{z} \quad (\text{B.19})$$

The functional variation goes as \sqrt{z} for $z \rightarrow 0$. The function is positive and the amplitude is of $O(\epsilon \ln \epsilon)$. For z large, the contribution to the integral from the region near $n = z$ is of $O(\epsilon/z^{3/2})$. Thus, we can use (B.18) or the original integral in the approximate form

$$F^*(\sqrt{z}, \epsilon) = \frac{1}{2\sqrt{z}} \int_0^z e^{n^2 g(n, \epsilon)} dn + O\left(\frac{\epsilon}{z^{3/2}}\right) \quad (\text{B.20})$$

We integrate by parts in (B.20) to obtain

$$F^*(\sqrt{z}, \epsilon) = \frac{1}{2\sqrt{z}} \left(-e^{-z^2} g(z, \epsilon) \right) + O\left(\frac{\epsilon}{z^{3/2}}\right) = O\left(\frac{\epsilon}{z^{3/2}}\right) \quad (\text{B.21})$$

Thus, we see that F^* decays faster than $1/\sqrt{z}$ for large z in contrast to Dawson's integral. We cannot evaluate F^* with (B.21) since we have already neglected terms of the same order.